

Donor–Acceptor Systems

Synthesis, Aromaticity and Photophysical Behaviour of Ferrocene- and Ruthenocene-Appended Semisynthetic Chlorin Derivatives

Taru Nikkonen,^[a] María Moreno Oliva,^[b] Stefan Taubert,^[a] Michele Melchionna,^[a]
Axel Kahnt,^{*[b]} and Juho Helaja^{*[a]}

Abstract: Two novel synthetic strategies to covalently link a metallocene electron-donor unit to a chlorin ring are presented. In one approach, pyropheophorbide *a* is readily converted into its 13¹-ferrocenyl dehydro derivative by nucleophilic addition of the ferrocenyl anion to the 13¹-carbonyl group. In another approach, the corresponding 13¹-pentamethylruthenocenyl derivative is synthesised from 13¹-fulvenylchlorin by a facile ligand exchange/deprotonation reaction with the [RuCp*(cod)Cl] (Cp* = pentamethylcyclopentadienyl; cod = 1,5-cyclooctadiene) complex. The resulting metallocene–chlorins exhibit reduced aromaticity, which was unequivocally supported by ring-current calculations based on

the gauge-including magnetically induced current (GIMIC) method and by calculated nucleus-independent chemical shift (NICS) values. The negative ring current in the isocyclic E ring suggests the antiaromatic character of this moiety and also clarifies the spontaneous reactivity of the complexes with oxygen. The oxidation products were isolated and their electrochemical and photophysical properties were studied. The ruthenocene derivatives turned out to be stable under light irradiation and showed photoinduced charge transfer with charge-separation lifetimes of 152–1029 ps.

Introduction

In photosynthesis, chlorophylls (Chls) have essential roles in light harvesting, energy transfer and charge separation.^[1] In artificial systems that mimic photosynthesis, Chl derivatives are often considered to be good electron donors and common systems for artificial photosynthesis feature conjugated Chls in the vicinity of electron acceptors.^[2–12] Less attention has been paid to examining Chl derivatives as electron acceptors,^[13,14] although in nature they also perform electron-accepting roles.^[1] In photosynthesis, the primary electron-transfer steps take place in the photosynthetic reaction centre, in which the excited dimer of Chl donates an electron to the pheophytin, resulting in a radical ion pair of the oxidised Chl dimer radical cation and reduced pheophytin radical anion.^[15]

To this end, metallocene derivatives of tetrapyrroles have been extensively used in various areas, such as light harvesting and solar-energy conversion,^[16–19] molecular devices,^[20] and

chemical sensors.^[21] Their excellent energy- and charge-transfer capability make them advantageous in mimicking photosynthetic processes.^[22] Strong electron donors, such as ferrocenes (Fc) and ruthenocenes (Rcs), are often conjugated in the vicinity of electron-accepting moieties^[23,24] or used as components to improve charge-transfer properties of biomimetic systems.^[25,26]

From a synthetic perspective, Fc moieties have been attached to various chromophores through well-established synthetic routes. For instance, several porphyrin–Fc conjugates have been prepared by means of metal-mediated cross-coupling reactions (e.g., Suzuki, Sonogashira) and Wittig-type reactions.^[27,28] In addition, a widely used and well-known route to porphyrins is the acid-catalysed condensation of (poly)pyrroles with aldehydes,^[29,30] thus, porphyrin–metallocenes can also be obtained through this approach by appropriate prefunctionalisation of the starting materials.

Another extensively applied approach for the synthesis of metallocenes is the metathesis of the lithium, sodium, or magnesium cyclopentadienyl salt with the metal.^[31] This method turned out to be very beneficial for the preparation of ring-fused compounds.^[32] As an example, Smith and co-workers have successfully synthesised ring-fused metallocenylporphyrins from cyclopentadienide-functionalised porphyrins by deprotonation with lithium diisopropylamide (LDA), followed by treatment with either [Ru(η^5 -C₅Me₅)Cl₂] or FeCl₂.^[33,34]

Fulvenes have also been shown to be useful starting materials in the synthesis of metallocenes. Reaction of fulvenes with lithium aluminum hydride, alkyllithium, or Grignard reagents leads to cyclopentadienyl complexes through addition or de-

[a] T. Nikkonen,⁺ Dr. S. Taubert, Dr. M. Melchionna, Dr. J. Helaja
Department of Chemistry, University of Helsinki,
P. O. Box 55,00014, University of Helsinki (Finland)
E-mail: juho.helaja@helsinki.fi

[b] Dr. M. Moreno Oliva,⁺ Dr. A. Kahnt
Department of Chemistry and Pharmacy &
Interdisciplinary Center for Molecular Materials (ICMM)
Friedrich-Alexander-Universität Erlangen-Nürnberg
Egerlandstraße 3, 91058 Erlangen (Germany)
E-mail: axel.kahnt@fau.de

[†] These authors contributed equally to this work.

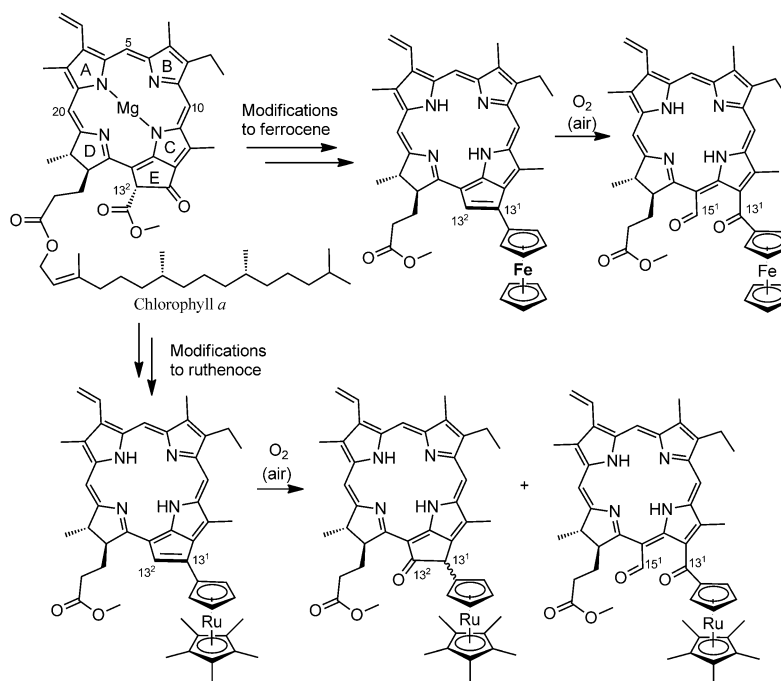
Supporting information for this article is available on the WWW under
<http://dx.doi.org/10.1002/chem.201501856>.

protonation.^[35,36] Alternatively, metallocenes can be prepared directly from fulvenes by reductive dimerisation with metallic calcium or transition-metal halides.^[37–40] In addition, it has been reported that ruthenium halide 1,5-cyclooctadiene (cod) reacts instantly with cyclopentadiene by dehydrohalogenation to yield the corresponding Rc derivative.^[41,42] In fact, this procedure has opened up several routes to Rcs, by reacting ruthenium complexes $[\text{Ru}(\eta^5\text{-C}_5\text{H}_5)(\eta^4\text{-C}_8\text{H}_{12})\text{X}]$ (C_8H_{12} = 1,5-cyclooctadiene; X = Cl, Br), $[\text{Ru}(\eta^5\text{-C}_9\text{H}_7)(\eta^4\text{-C}_8\text{H}_{12})\text{Cl}]$ (C_9H_7 = indenyl) and $[\{\text{Ru}(\eta^5\text{-C}_5\text{Me}_5)\text{Cl}\}_4]$ with cyclopentadienes and even with 3-vinyl-1-cyclopropenes. Moreover, mono-substituted cyclopentadienyl ruthenium complexes have been obtained from the reactions of 6-substituted fulvenes with $[\text{RuHCl}(\text{PPh}_3)_3]$.^[43]

Metallocene-derived porphyrins, especially Fc-appended porphyrins, have been of high interest due to their well-known redox and photochemistry.^[27] Fcs are reputed to possess high stability and undergo reversible one-electron ($1e^-$) oxidation in nonaqueous media. In contrast, the redox chemistry of Rc derivatives is more complicated because it depends on the solvent, supporting electrolyte and substituents in the cyclopentadienyl rings.^[44–47] In various cases, Rcs have been reported to undergo irreversible two-electron ($2e^-$) oxidations.^[48,49] However, reversible $1e^-$ oxidation occurs in molten salts^[50] or when noncoordinating electrolyte and noncoordinating solvent are used.^[51] Alternatively, reversible $1e^-$ oxidation has also been obtained by introducing steric hindrance; for instance, decamethylruthenocene^[52] $[\text{Ru}(\eta^5\text{-C}_5\text{Me}_5)_2]$, indenyl ligand containing^[52] $[\text{Ru}(\eta^5\text{-C}_5\text{Me}_5)(\eta^5\text{-indenyl})]$ and octamethyl[3]ruthenocenophane^[53] underwent reversible $1e^-$ oxidation. Moreover, Smith and co-workers observed reversible $1e^-$ oxidation for their ruthenocenoporphyrin, which implied that the porphyrin macrocycle acted as a stabilising ligand for the singly oxidised Rc cation.^[33,34]

Several studies have shown that Fc can effectively quench the singlet excited state of porphyrin through photoinduced electron transfer.^[18,19,23,54] Moreover, the groups of Kadish, Fukuzumi and Sessler studied (pentamethylcyclopentadienyl)ruthenium π complexes of metalloporphyrins and observed photoinduced electron transfer from the Rc unit to the singlet excited state of the metalloporphyrin.^[55–57] Similarly, (pentamethylcyclopentadienyl)ruthenium π complexes and sitting-atop metalloporphycenes also underwent electron transfer.^[54–57]

To the best of our knowledge, there are no examples in the literature of a Chl derivative attached to any metallocene.



Scheme 1. Routes to auto-oxidised metallocene chlorins derived from Chl *a*.

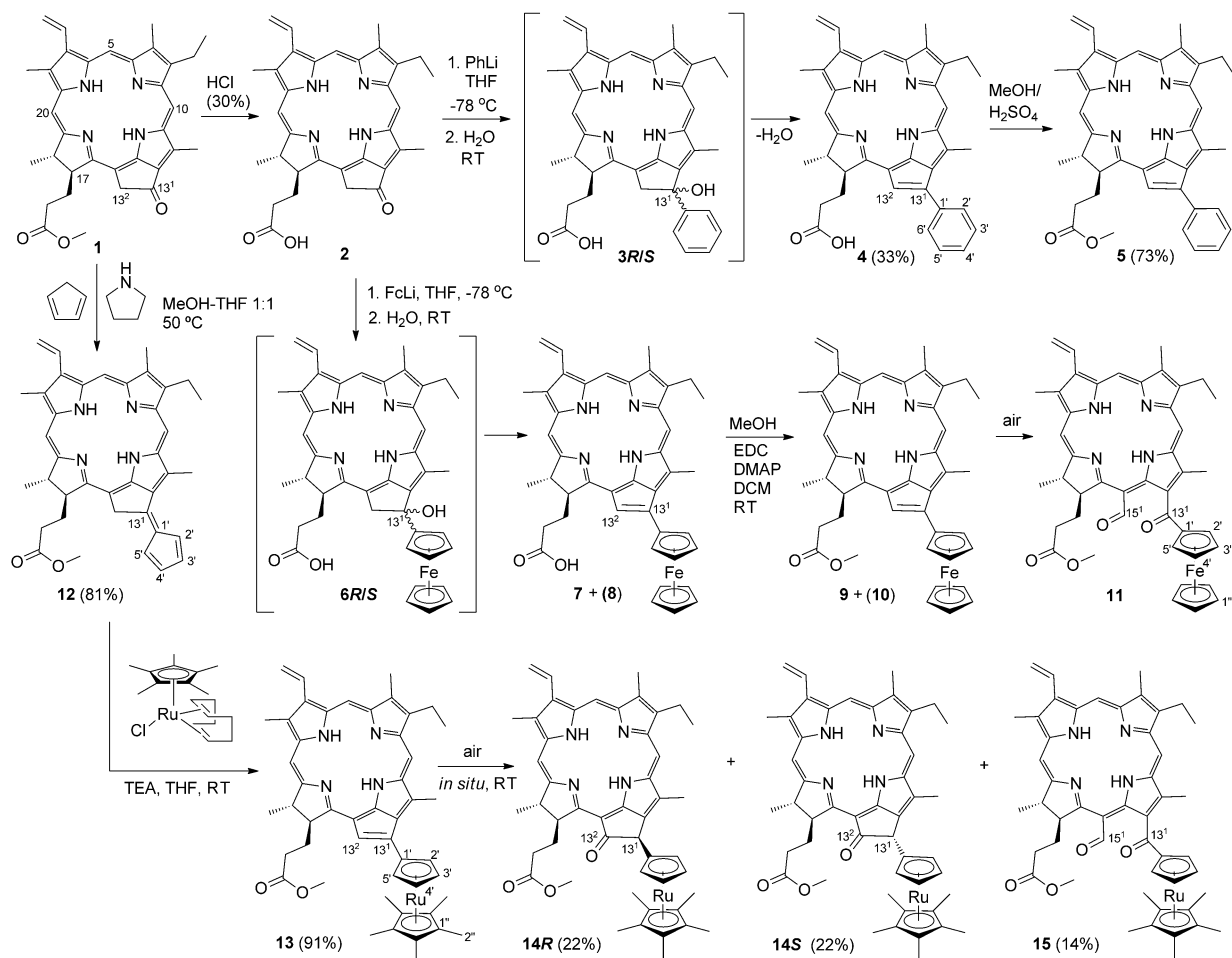
Herein, we have demonstrated two distinct synthetic pathways to unprecedented metallocene-appended pyropheophorbide *a* methylester derivatives. In our approach, the chlorin macrocycle was conjugated at the 13¹-position with a metallocene (either $[\text{Fe}(\eta^5\text{-C}_5\text{H}_5)(\eta^5\text{-C}_5\text{H}_4)]$ or $[\text{Ru}(\eta^5\text{-C}_5\text{Me}_5)(\eta^5\text{-C}_5\text{H}_4)]$; Scheme 1). The Fc–chlorin complex was formed through the addition of ferrocenyllithium to 13¹-carbonyl, whereas the synthesis of the Rc analogue relied on the use of 13¹-fulvene-derivatised chlorin as a starting material. The chemical properties and tendency of the conjugated ring E to oxidation (Scheme 1) are also studied and discussed. The air-stable oxidation products were characterised and investigated by means of photo-physical and electrochemical studies.

Results and Discussion

Synthesis and characterisation

The synthesis of all molecules is presented in Scheme 2. Chl *a* was extracted and purified from *Spirulina pacifica* and converted into pyropheophorbide *a* methylester (**1**), which was used as a starting material for all the syntheses.^[58]

At the start, we synthesised phenyl-substituted chlorin derivative (**5**) as a reference for all studied chlorin–metallocenes. It was shown previously that alkylation of the chlorin 13¹-keto group could be carried out by McMurry coupling,^[59] Knoevenagel condensation,^[60] or treatment with organolithium reagents.^[61] Herein, we opted for the last approach, with prior acid hydrolysis of **1**^[62] to give pyropheophorbide *a* (**2**) to suppress unwanted side reactions (i.e., direct alkylation of the 17³-ester or Claisen reaction with the 13²-anion).^[63] The addition of



Scheme 2. Synthetic pathways from **1**: HCl-catalysed ester hydrolysis of **1** to **2**, followed by nucleophilic addition of PhLi and in situ hydrolysis to give phenylchlorin acid **4**, which was esterified to give **5**. Analogous nucleophilic addition of FcLi to **2**, hydrolysis and esterification to give **9** and **10**. Ruthenocenylchlorin **13** prepared mixing fulvene **12** with [RuCp*(cod)Cl] and triethylamine (TEA). Fulvene **12** is condensed from **1** and cyclopentadiene under base catalysis. Fc chlorin **9** and Rc chlorin **13** both undergo auto-oxidation (**9** → **11**; **13** → (*R/S*)-**14** and **15**). EDC = *N*-(3-dimethylaminopropyl)-*N*-ethylcarbodiimide, DMAP = 4-dimethylaminopyridine.

phenyl lithium to **2** and protonation of the as-formed alkoxide by addition of water gave the tertiary alcohol (*R/S*)-**3**, which spontaneously dehydrated during purification on a silica column to give alkene **4** (yield 33%, from **2**). Esterification of **4** in acidic methanol gave the final product **5** in 73% yield after flash column chromatography.

In an analogous manner, we obtained our second target molecule, 13¹-ferrocenylchlorin (**7**), by treating **2** with ferrocenyllithium, which was prepared by metal-halogen exchange of commercially available bromoferrocene and *n*-butyllithium.^[64] Also in this case, alkylation of the 13¹-carbonyl was followed by dehydration, by chromatography on SiO₂, leading to **7**. However, despite many purification efforts, a comparable amount of an inseparable ferrocenyl-derived side product, denoted as **8**, was also observed. Unfortunately, any further efforts to separate the mixture of **7** and **8** led to decomposition of the compounds. The NMR spectra (see Figures S8–S13 in the Supporting Information) and HRMS (ESI) analysis of the mixture indicated that the latter was not the (*R/S*)-**6** intermediate, but some kind of chlorin Fc derivative without a double bond in the isocyclic ring. Next, we treated the mixture of **7**

and **8** to mild esterification conditions, by using EDC as a cross-linking reagent and DMAP as a catalyst, to transform **7** into the corresponding methyl ester **9**. With this treatment, unidentified chlorin **8** was transformed into chlorin **10** without the formation of characteristic methyl ester NMR resonances (see Figures S14–S20 in the Supporting Information), but with the appearance of exceptionally high-field-shifted NH signals. When flash chromatography was carried out under air, compounds **9**, **10** and **11** were obtained. In particular, air-sensitive compounds **9** and **10** could be collected only as a mixture, whereas the auto-oxidised red product **11**, which formed upon flash chromatography on SiO₂, turned out to be stable and was successfully isolated (yield: 12%, calculated from **2**) and characterised. Instead, when flash chromatography was carried out under a flow of argon and the eluents were carefully deoxygenated by prior bubbling with argon, only a mixture of **9** and **10** were obtained. By prolonged chromatography under argon, we eventually succeeded in isolating small amounts of Fc derivative **9** for characterisation, although the vast majority of **9** and **10** remained as an inseparable mixture.

As a parallel synthetic approach to chlorin metalloenes, we developed an alternative methodology that utilised a fulvene route, allowing the synthesis of different derivatives when combined with metallocyclopentadienes (Scheme 2). Inspired by the work of Stone and Little,^[65] who reported that fulvenes could be conveniently obtained from the corresponding ketones and cyclopentadienes in methanol by using pyrrolidine as a base, we explored this route as a possible pathway. To our delight, we successfully obtained the desired product **12** from **1**, in 81% yield after column chromatography, by treatment with freshly distilled cyclopentadiene in the presence of pyrrolidine. To overcome problems associated with the insolubility of chlorin **1**, we adjusted the experimental conditions and carried out the reaction in a 1:1 mixture of MeOH/THF.

In our synthetic strategy, we expected the reaction to proceed through an initial coordination of the fulvene moiety by facile ligand exchange with the labile cod ligand in the ruthenium(II) precursor followed by metallocene formation in the presence of an appropriate base.^[66–68] To our pleasure, when fulvene **12** was treated with $[\text{Ru}(\eta^5\text{-C}_5\text{Me}_5)(\eta^4\text{-C}_8\text{H}_{12})\text{Cl}]$ in the presence of TEA, 13¹-pentamethylruthenocenylyl derivative **13** was successfully synthesised in excellent yield (91%) after chromatographic purification. The use of TEA was essential to capture HCl released over the course of the reaction, which otherwise interfered and led to decomposition. The reaction was also performed in an NMR tube in $[\text{D}_8]\text{THF}$ and monitored by ¹H NMR spectroscopy, which revealed that the chlorin–fulvene starting material was converted rather cleanly into the Rc (see Figure S34 in the Supporting Information). The air-sensitive Rc (**13**) was instantly purified by filtration through a silica pad under argon and characterised immediately. Exposing **13** to air in situ by stirring at room temperature in the dark led to concomitant oxidation to stereoisomers (*R/S*)-**14** and the doubly oxidised product **15**. All of the oxidised chlorin–Rcs were stable under air and were successfully separated by flash chromatography.

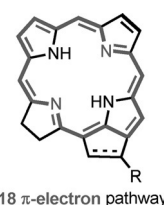
For (*R*)- and (*S*)-**14**, the *R/S* stereochemistry was determined by utilising NOESY NMR spectroscopy experiments, which showed a NOE correlation between 5'-H of the cyclopentadienyl ring and 17¹-H of the aliphatic tail of the chlorin macrocycle for the first eluted product (see Figures S53–S54 in the Supporting Information). This form corresponded to the (*R*)-**14**-stereoisomer, in which the Rc moiety was oriented upwards from the chlorin plane (on the same side as the 17-propionic ester residue). As expected, the NOE correlation between 5'-H and 17¹-H was not observed for the second eluted product (*S*)-**14**. The results were in accordance with molecular geometries optimised by DFT calculations at the TPSS/def2-SVP level, including dispersion corrections with the D3 model and BJ-damping with the COSMO solvation model for CHCl_3 , in which the spatial distance between protons 5'-H and 17¹-H was 2.8 Å for (*R*)-**14**, whereas the corresponding distance for (*S*)-**14** (see Figure S65 in the Supporting Information) was 4.8 Å.

Commonly, derivatives **5**, **9** and **13** have a C₁₃1=C₁₃2 bond in ring E, which makes these compounds labile. Extensive CHl studies by Hynninen and co-workers demonstrated that the presence of a double bond at 13¹–13² position perturbed the

delocalised π system and increased steric strain in the periphery of the molecule.^[69–71] The electron-rich metallocene unit further destabilises this 13¹–13² position, since both Fc- and Rc-appended chlorins containing the 13¹=13² bond are remarkably more sensitive to oxidation than the corresponding phenyl-substituted chlorin, **5**, which survives flash chromatography in standard conditions under air. Interestingly, both ferrocenyl- and ruthenocenylyl-appended chlorins **9** and **13** afforded similar oxidation products (**11** and **15**) with a ketone bridge in the 13¹-position and aldehyde in the 15¹-position. In comparison, Dolphin and Ma reported that exposure of a pyropheophorbide *a* methylester derivative with the 13¹=13² bond and a methyl ester in the 13²-position to air and sunlight oxidatively cleaved the double bond, affording an aldehyde in the 13¹-position and a ketone in the 15¹-position.^[72,73] In the case of ruthenocenylyl–chlorin, the two stereoisomers, (*R*)- and (*S*)-**14**, were also obtained. In relation to metallocenes, Li et al. previously reported a similar type of selective oxidation of a neighbouring cyclopentadiene in the Fc into cyclopentenone, which took place in air in the dark, and was clearly promoted by the ferrocenyl group.^[74]

Ring-current studies

The formation of an additional 13¹=13² bond in products **5**, **9** and **13** potentially extends the conjugation pathway of the chlorin macrocycle. This suggests that the modified chlorin macrocycle possesses not only the characteristic aromatic 18 π -electron conjugation pathway, but is also accompanied by some other conjugation pathways, in which the formed double bond might be involved (Scheme 3). In general, aromatic compounds show the ability to sustain an induced ring current, namely, a diatropic ring current. The tendency of aromaticity is commonly manifested in the ¹H NMR spectra, which show deshielding for outer-ring protons and shielding for inner-ring protons in aromatic compounds. The ¹H NMR spectra of **1**, **5**, **9** and **13** are shown in Figure 1. Visibly, the shielding of the outer-ring protons is increased in chlorins **5**, **9** and **13** (and also in chlorins **4** and **7**; see Figures S1 and S8 in the Supporting Information), which can be attributed to a weakening of the diatropic ring current. The most significant upfield shifts are observed for the methine protons (5-H, 10-H and 20-H). Also, protons 2¹-, 3¹-, 3²-, 7¹-, 8¹-, 8²-, 12¹-, 17-, 18- and 18¹-H show moderate upfield shifts. Notably, NH protons experience significant deshielding and are shifted prominently downfield. Similar spectral changes and a decrease in aromaticity have been reported for both the free base and central metal, including chlorin derivatives with a 13¹=13² bond.^[71,75]



Scheme 3. Classic 18 π -electron delocalisation pathway (gray) for a chlorin macrocycle. Modified chlorins with the 13¹=13² bond show weakened ring currents, which indicates different strengths of or pathways for conjugation.

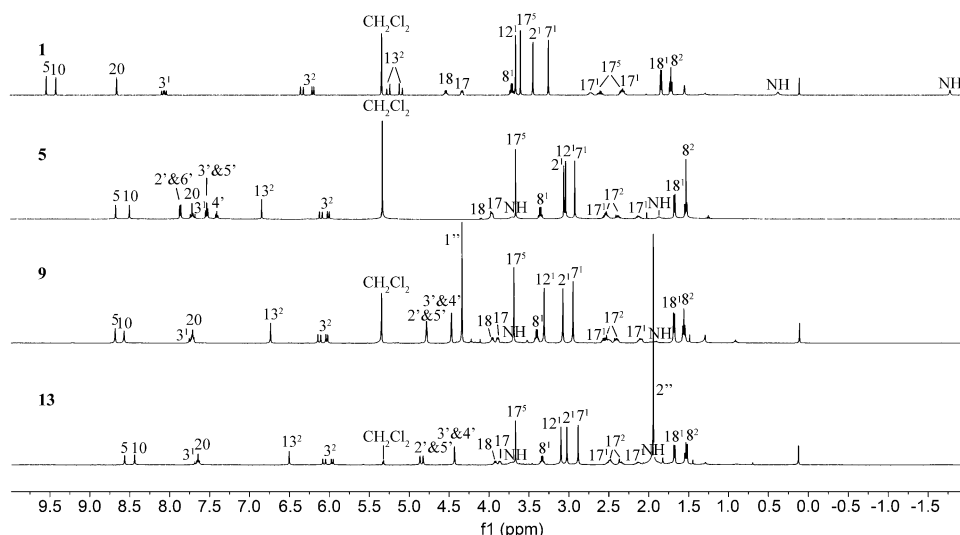


Figure 1. Overlay of ^1H NMR spectra of **1**, **5**, **9** and **13** in CD_2Cl_2 .

A related theoretical examination with the gauge-including magnetically induced current (GIMIC) method offered a convenient tool to gain an insight into the aromaticities of the studied chlorins. The ring-current pathways and strengths for chlorins **1** and **5** are depicted in Figures 2 and 3, respectively. The ring-current strengths were calculated for the structures optimised at the TPSS-D3/def2-SVP level. In **1**, the present calculations at the B3LYP/def2-SVP level show a diatropic macrocyclic ring current of 23 nAT^{-1} circulating around the macrocycle. This is similar to the macrocyclic ring-current strength in plain *trans*-chlorins, which is 20 or 24 nAT^{-1} , depending on which two nitrogen atoms are protonated, as calculated at the B3LYP/def2-TZVP level.^[76] In chlorin **5**, the ring-current strength is slightly more than half of that in **1**, or 13 nAT^{-1} . This is almost the same as the ring-current strength in benzene, which is

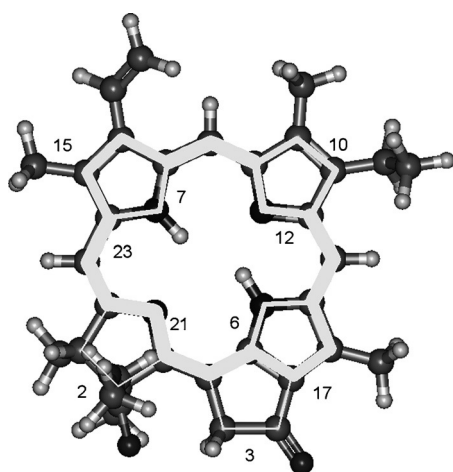


Figure 2. Ring-current pathways in chlorin **1**. The number indicates the total ring-current strength passing through selected bonds. The macrocyclic ring-current strength is 23 nAT^{-1} . Positive values and the white path indicate diatropic ring-current pathways.

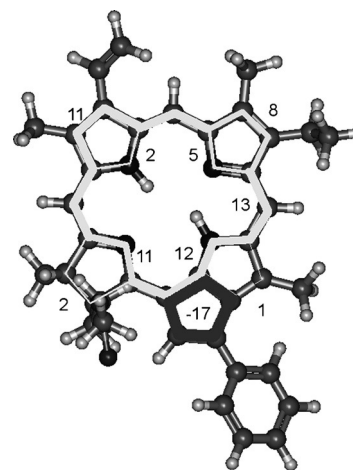


Figure 3. Ring-current pathways in chlorin **5**. The number indicates the total ring-current strength passing through selected bonds. The macrocyclic ring-current strength is 13 nAT^{-1} . Positive values and the white path indicate diatropic ring-current pathways. The negative value (-17 nAT^{-1}) and gray path shows the paratropic ring current of the antiaromatic cyclopentadienyl ring.

In **1**, no local ring currents are found in the pyrrole or isocyclic ring E, but the macrocyclic current is split at the rings, so that part of the current flows along the inner pathway and part along the outer (Figure 2). In **1**, the conjugation pathway along the outer route of the isocyclic ring is interrupted because the addition of the carbonyl group at the 13^1 -position changes the hybridisation of the 13^2 -carbon to sp^3 . This effectively hinders the current flow from passing along the 13^1 – 13^2 bond and instead almost all current passes through the inner route. The current along the outer edge of the cyclopentene ring is only 3 nAT^{-1} . In **5**, the isocyclic ring E localises a considerable paratropic ring current of -17 nAT^{-1} , which indicates the antiaromatic character of that ring (Figure 3). The NICS(0) value at the centre of the cyclopentadienyl ring is $+22.1$, which is in

line with an antiaromatic character. Thus, the magnetic criterion for aromaticity agrees with the observation that the $13^1=13^2$ bond is very reactive. The strong paratropic ring current in ring E of **5** effectively hinders the macrocyclic current from passing through the $13^1=13^2$ bond, and therefore, prevents the 20π -electron delocalisation pathway. This is very similar to what was recently observed for thieno-bridged porphyrins.^[78] Also, at pyrrole ring C, there is a qualitative difference in the current localisation in **1** and **5**. In **1**, the macrocyclic current is split at the pyrrole ring, so that 17 nAT^{-1} passes through the outer route and 6 nAT^{-1} passes through the protonated nitrogen atom. In the less aromatic chlorin **5**, practically all of the current passes through the inner route at the protonated nitrogen atom, whereas only 1 nAT^{-1} passes through the outer path. At the other pyrrole rings in **1**, the macrocyclic ring current is split in a similar manner as that seen for porphyrins previously. Characteristically, the main fraction of the current flows along the outer part of the N-protonated pyrrole rings (A and C). The flow is more equally divided along the inner and outer paths at nonprotonated pyrrole rings, and the larger part of the current flows along the inner path. In **5**, splitting of the macrocyclic ring current at the pyrrole rings does not completely follow this pattern, as shown in Figure 3.

Photophysical studies

To elucidate the electronic features of the novel metallocene chlorins, photophysical investigations were performed by means of steady-state and time-resolved absorption and emission spectroscopy. Conjugated **9** and **13** were extremely sensitive to both light and oxygen and could not be studied photophysically. Chlorin **5** was stable in air when kept in the dark, but decomposed during photophysical measurements.

The steady-state absorption spectra of **1**, **11**, (*R*)-**14**, (*S*)-**14** and **15** are shown in Figure 4a. The absorption spectrum of reference **1** shows characteristic Soret and Q_y band maxima at 411 and 669 nm, respectively. In comparison to reference **1**, the Q_y bands of **11** and **15** are both remarkably redshifted, and appear at 698 and 700 nm, respectively, whereas the redshifts of the Soret bands are indistinguishable, at 412 and 413 nm, respectively. The absorption spectra of the two stereoisomers (*R*)- and (*S*)-**14** are almost uniform, and in comparison to **1** the Soret and Q_y band maxima are blueshifted to $\lambda = 400$ and 666 nm, respectively.

The fluorescence spectra of the corresponding samples with equal optical densities at the excitation wavelength 403 nm were measured. Surprisingly, excitation of either **11** or **15** at 403 nm resulted in fluorescence spectra with emission maxima at 675 and 674 nm, respectively, which means at higher energies than the energetically lowest absorption band (Q_y). For the ferrocenylchlorin **11**, photochemical decomposition was clear, since the absorption spectrum of the compound changed gradually after each fluorescence measurement. The ruthenocylchlorin **15** did not show changes in its absorption spectrum after fluorescence measurement, presumably due to better stability. However, the unusual fluorescence maximum of **15** means that the fluorescence arises from photochemical

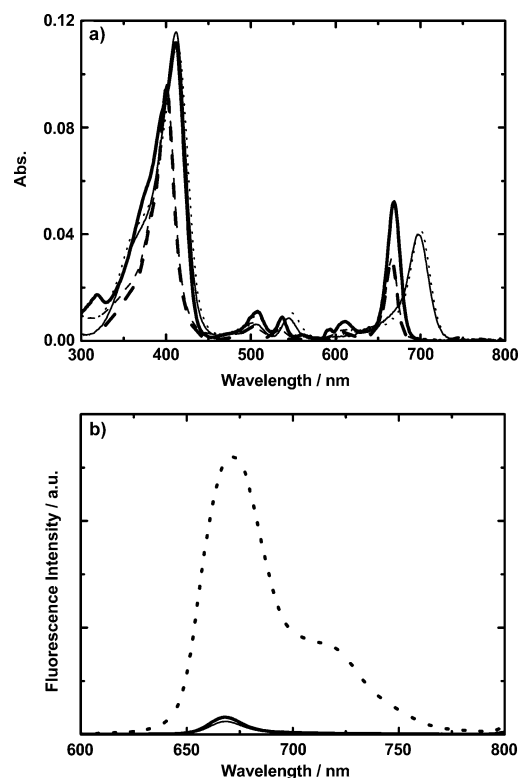


Figure 4. a) Absorption spectra of **1** (—), **11** (---), (*S*)-**14** (- - - -), (*R*)-**14** (- · - · -) and **15** (· · · · ·) in THF. b) Fluorescence spectra of **1** (· · · · ·), (*R*)-**14** (—) and (*S*)-**14** (---) in THF (excitation at $\lambda = 403$ nm).

products that are similar to those observed in the case of **11**. The better stability of **15** than **11** can be explained in terms of the electron-donating ability of the methyl groups in the pentamethylcyclopentadienyl ligand in **15**. This results in stronger bonding and increased steric bulk than that of the cyclopentadienyl ligand in **11**. The fluorescence spectra of photochemically stable **1**, (*R*)-**14** and (*S*)-**14** are included in Figure 4b. Reference **1** shows an emission maximum at 671 nm, whereas compounds (*R*)-**14** and (*S*)-**14** both show significantly quenched fluorescence with maxima at 666 nm.

Fluorescence quantum yields (Φ_f) and fluorescence lifetimes (τ) of photochemically stable **1**, (*R*)-**14** and (*S*)-**14** were determined at an excitation wavelength of 403 nm (Table 1). The fluorescence quantum yields of pentamethylruthenocenylchlorins were significantly decreased in comparison with reference **1**; this should be related to the involvement of a charge-transfer process. The fluorescence lifetimes have been measured to characterise the singlet-singlet pathway for the deactivation process. The experimental results are analysed and best described by a monoexponential decay in the case of reference **1**, and biexponential decay in ruthenocenylchlorins derivatives (*R*)-**14** and (*S*)-**14**. In the presence of the Rc unit, a short-lived component is observed ($\tau = 0.2/0.3$ ns). The long-lived component is best explained by impurities of chlorin derivatives remaining from the synthetic procedure.

Next, we performed electrochemical experiments to obtain information on electron-transfer reactions and redox multi-stage mechanisms. Reference **1** shows amphoteric redox be-

Table 1. Soret and Q_y band maxima in the UV/Vis absorbance spectra and the emission maxima of the fluorescence spectra of **1**, **11**, (*R*)-**14**, (*S*)-**14** and **15**. Fluorescence lifetimes (τ) determined by time-correlated single photon counting ($\lambda_{\text{exc}}=403$ nm and $\lambda_{\text{em}}=670$ nm) and fluorescence quantum yields (Φ_F) ($\lambda_{\text{exc}}=403$ nm) in THF are also given.

	Absorption [nm]		Fluorescence maxima [nm]	τ_1 [ns] (%)	τ_2 [ns] (%)	Φ_F
	Soret	Q_y				
1	411	669	671	6.9 (100)	–	0.13
11	411	697	[a]	[a]	–	[a]
(<i>R</i>)- 14	400	666	668	0.2 ^[b] (76)	2.9 (24)	0.006
(<i>S</i>)- 14	400	666	668	0.3 ^[b] (80)	3.0 (20)	0.008
15	413	700	[a]	[a]	[a]	[a]

[a] Could not be determined due to decomposition during measurements. [b] These values are at the lower time resolution limit of our fluorescence lifetime setup; from transient absorption, values of 68 and 72 ps for (*R*)- and (*S*)-**14**, respectively, were obtained as lifetimes for the first singlet excited states.

haviour in the cyclic voltammogram (Table S1 in the Supporting Information), which consists of two reversible oxidations at +0.61 and +0.91 V and one reversible reduction at –1.43 V; this is consistent with redox chemistry reported for similar chlorin derivatives.^[79] The inclusion of the Rc unit in (*S*)-**14** and **15** results in the appearance of lower oxidation potentials in the molecules due to the strong electron-donating character of Rc. For (*S*)-**14**, the first reversible oxidation appears at +0.31 V and arises from the Rc unit, whereas the second reversible oxidation appears at +0.64 V and results from oxidation of the chlorin macrocycle. The reversible reduction of the chlorin macrocycle is observed at –1.50 V. In **15**, two irreversible oxidations are observed: the first one at +0.38 V arises from Rc and the second oxidation at +0.63 V arises from the chlorin macrocycle, in addition to a shoulder at +1.15 V. Two reversible reductions of the chlorin macrocycle are observed at –1.24 and –1.49 V. The electrochemical band gap decreases in the studied molecules as follows: 2.04 (**1**), 1.81 ((*S*)-**14**) and 1.62 V (**15**). Spectroelectrochemical experiments provided the fingerprint of the successfully reduced chlorin macrocycle. In the case of **15**, we increased the applied potential from 0.0 to 1.2 V and down to –1.2 V. The resulting differential spectra show characteristic maxima at $\lambda=529$, 578, 610 and 663 nm and bleaching at 509, 550, 640 and 701 nm (strong; see Figure S62 in the Supporting Information). It must be highlighted that there is a new maximum at 425 nm in the oxidation scan, which shifts to 433 nm at higher potentials. In the reduction data, a weak peak at 438 nm is observed, which is also red-shifted at higher potentials. Going back step by step in the opposite direction, we observed irreversible behaviour of the signature, in accordance with electrochemical data. However, in the case of (*S*)-**14**, two new maxima at 420 and 700 nm appear in both oxidation and reduction data, whereas only a decrease in intensity is observed at higher potentials (see Figure S61 in the Supporting Information).

Conclusive information on the nature of the interactions between the chlorin and Rc units came from transient absorption spectroscopy. Photoexcitation of **1** at 387 nm in THF reveals the formation of the chlorin singlet excited state with transient absorption maxima at 460, 485, 525 and 580 nm accompanied by a shoulder around 620 nm and transient bleaching at 670

and 725 nm (see Figure 5). These features decay slowly on the picosecond timescale ((6755 ± 1707) ps) to the energetically lower-lying triplet excited state by intersystem crossing (ISC). The rate of ISC into the first excited triplet state is in agreement with the observed fluorescence lifetime, that is, 6.9 ns, and consistent with previously reported fluorescence lifetimes and ISC rate constants for free-base chlorins.^[80–82] The character-

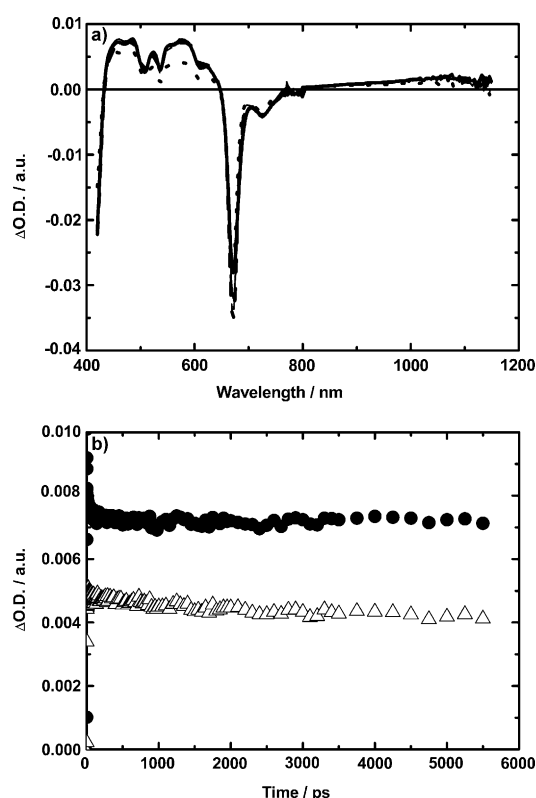


Figure 5. a) Femtosecond transient absorption spectra of **1** in argon-saturated THF: **1** (—), 10 (—), 100 (----), 1000 (----) and 5500 ps (••••) after excitation at $\lambda=387$ nm. b) Corresponding time absorption profiles at $\lambda=450$ (●) and 490 nm (△).

istic transient absorption bands of the corresponding triplet state are located around 445, 485, 525, 575 and 665 nm accompanied by transient bleaching around 670 and 725 nm (see Figure S63 in the Supporting Information). Also, the lifetimes of the triplet excited state are quenched by molecular oxygen, namely, (175 ± 21) μ s and (47 ± 2) ns in the absence and presence of molecular oxygen, respectively.

Concerning chlorin with the attachment of a Rc unit (**15**), the transient absorption spectrum of the first excited singlet state shows transient absorption bands with maxima at 460,

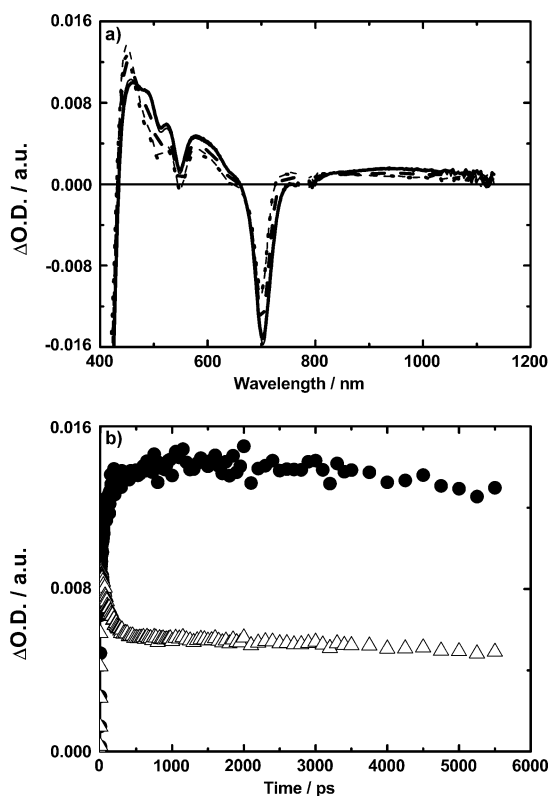


Figure 6. a) Femtosecond transient absorption spectra of **15** in argon-saturated THF: **1** (—), **10** (---), **100** (.....), **1000** (-.-.-) and **5500** ps (.....) after excitation at $\lambda = 387$ nm. b) Corresponding time absorption profiles at $\lambda = 450$ (●) and 490 nm (△).

525, 575 and 950 nm and a shoulder around 490 nm, accompanied by a transient minimum at 700 nm (Figure 6). These transient absorptions decay rapidly within 1 ps to give rise to a new set of transient absorption bands with maxima around 450, 520, 580 and 900 nm together with transient minima around 510, 550 and 700 nm. This new transient absorption is in agreement with spectroelectrochemical measurements (see Figure S62 (right, electrochemical reduction) in the Supporting Information) and values in the literature assigned to the charge-separated state,^[55] which shows a lifetime of (152 ± 5) ps. The decay of the charge-separated state gives rise to a new set of transient absorption with maxima at 445, 530, 600 and 760 nm and transient minima at 510, 550 and 700 nm. This transient absorption matches well with Chl *a* triplet state, known in the literature.^[83]

The lifetime of the first excited triplet state of **15** was obtained from nanosecond transient absorption measurements and fitted to (241 ± 7) and (65 ± 0.5) ns in the absence and presence of molecular oxygen, respectively (see Figure S64 in the Supporting Information). Femto- and nanosecond laser flash photolysis analyses show that photoinduced electron transfer from the Rc unit (acting as an electron donor) to the singlet excited state of chlorin (acting as an electron acceptor) takes place efficiently after photoexcitation followed by decay to the triplet state of chlorin. Another important aspect to which attention should be paid is that the lifetime of the trip-

let state is dramatically shortened in compound **15**, compared with reference compound **1**. This indicates that the Rc moiety has ability to quench the triplet state formed. In comparison, Fcs are also known as classical quenchers of the lowest energy excited states, generally the triplet state.^[19,54]

As far as the oxidised Rc derivatives (*R*)- and (*S*)-**14** are concerned (Figure 7), both give almost identical transient absorption spectra upon laser excitation at 387 nm (see Figure 7a and c) with maxima at 485, 515 and 550 nm and shoulders at 460 and 585 nm, as well as minima at 500, 530 and 670 nm, which mirror the ground-state absorption. This is assigned to the first excited singlet state of the chlorin derivative, which decays with a lifetime of (68 ± 9) ps for (*R*)-**14** and (72 ± 10) ps for (*S*)-**14** into a new set of transient absorptions with maxima at $\lambda = 460, 520, 545$ and 620 nm and minima at 500, 535 and 700 nm. This transient absorption relates to the charge-separated state, which decays within (938 ± 117) ps for (*R*)-**14** and (1029 ± 135) ps for (*S*)-**14** into the corresponding triplet manifold, showing transient absorption maxima at 445, 520 and 550 nm and minima at 500, 530 and 700 nm (see Figure 7a and c). The lifetimes of the triplet state are (268 ± 9) and (71 ± 5) ns in (*R*)-**14** and (289 ± 22) and (79 ± 4) ns in (*S*)-**14**, in the absence and presence of molecular oxygen, respectively.

Frontier molecular orbital calculations

Frontier molecular orbitals (FMOs) were calculated for all minimum-energy geometries (see the Supporting Information). For molecules of photophysical interest, namely, compounds (*R*)-**14**, (*S*)-**14** and **15**, these orbitals are illustrated in Figure 8. In each structure, the HOMOs are localised in the Rc unit and the LUMOs are correspondingly in the chlorin macrocycle. Similar localisation of FMOs could also be observed for **11** (see the Supporting information). In comparison, reference compound **1** shows both HOMO and LUMO delocalised over the chlorin macrocycle (see the Supporting information). Meanwhile, the compounds with an extended conjugation pathway, namely, compounds **5**, **9** and **13**, show delocalised HOMOs and weakly localised LUMOs (see the Supporting information). The localised frontier orbitals of (*R*)-**14**, (*S*)-**14** and **15** suggest that the Rc unit and chlorin macrocycle act in each molecule as the electron donor and acceptor, respectively. The calculated HOMO–LUMO gaps for the photophysically studied compounds decrease as follows: 1.608 (**1**), 1.314 ((*S*)-**14**), 1.300 ((*R*)-**14**) and 1.091 eV (**15**). It is noteworthy that the electrochemical band gap also decreased in the same order for these molecules.

Conclusion

Novel metallocene-functionalised chlorins were synthesised by two distinct synthetic routes to functionalise the 13¹-keto group of **1**: 1) by direct alkylation with the Fc anion and 2) by its addition reaction with cyclopentadiene to give the fulvene intermediate, which was converted into the Rc by treating it with [RuCp*(cod)Cl] complex.

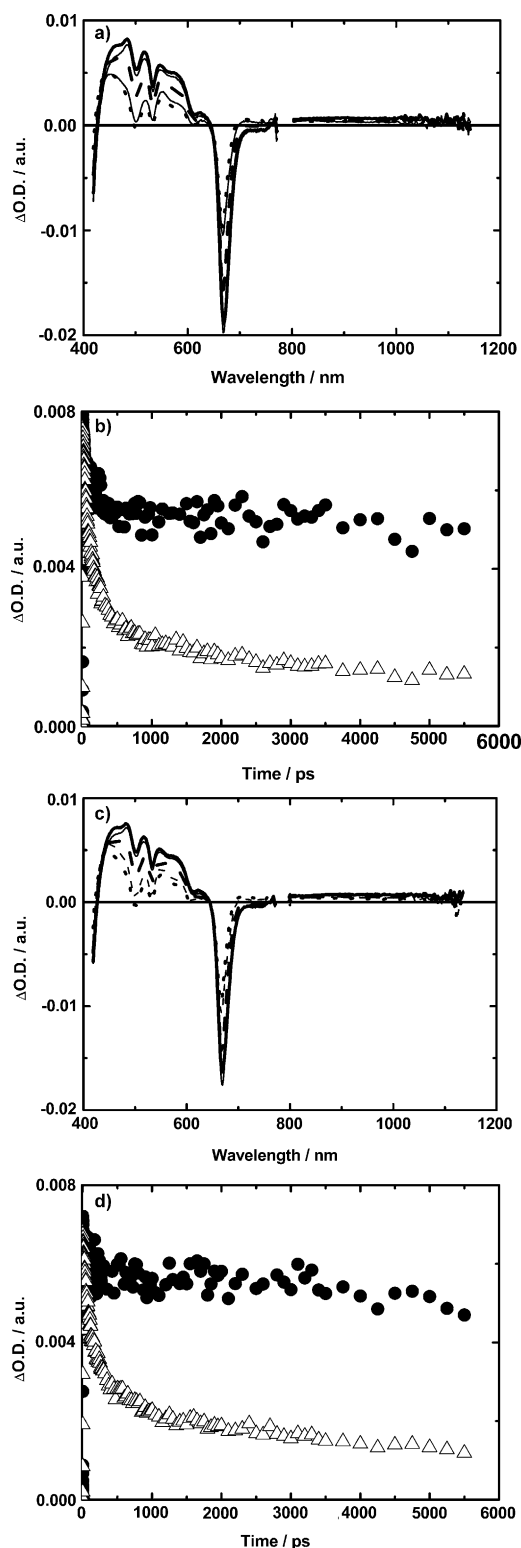


Figure 7. a) Femtosecond transient absorption spectra of (*R*)-14 in argon-saturated THF: 1 (—), 10 (—), 100 (-----), 1000 (-----) and 5500 ps (.....) after excitation at $\lambda = 387$ nm. b) Corresponding time absorption profiles at $\lambda = 450$ (●) and 490 nm (Δ). c) Femtosecond transient absorption spectra of (*S*)-14 in argon-saturated THF: 1 (—), 10 (—), 100 (-----), 1000 (-----) and 5500 ps (.....) after excitation at $\lambda = 387$ nm. d) Corresponding time absorption profiles at $\lambda = 450$ (●) and 490 nm (Δ).

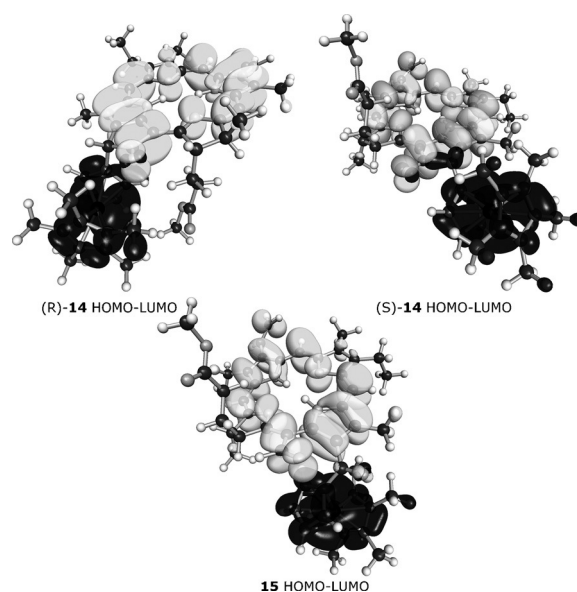


Figure 8. TPSS-D3/def2-SVP geometry-optimised structures and FMOs of (*R*)-14, (*S*)-14 and 15 (black: HOMO; white: LUMO). Isosurface value: 0.02.

The NMR spectra of the synthesised phenyl-, Fc- and pentamethylruthenocene-appended chlorins (**5**, **9** and **13**) indicated the formation of an additional double bond in the E ring, which disturbed the chlorin 18π -aromatic conjugation pathway, as denoted by chemical shifts. In the case of metallocene-chlorins **9** and **13**, the double bond formed turned out to be spontaneously reactive with molecular oxygen, resulting in conjugated products (**9** \rightarrow **11**; **13** \rightarrow (*R/S*)-**14** and **15**). The phenyl-appended derivative (**5**) showed better stability in air, but decomposed under normal light.

The ring-current pathways of chlorins **1** and **5** were investigated by GIMIC. There was a strong paratropic ring current in the ring E of chlorin **5**, which prevented the macrocyclic current from passing through the $13^1=13^2$ bond. Despite an overall aromatic macrocyclic 18π -electron current pathway, the ring current in chlorin **5** was only about half as strong as that in **1**. The NICS(0) values were in agreement with the obtained macrocyclic ring-current strengths.

The photophysical properties of ferrocenylchlorin **11** and ruthenocenylchlorins (*R*)-**14**, (*S*)-**14** and **15** were investigated. A comprehensive study was accomplished for (*R*)- and (*S*)-**14** because these compounds were photochemically stable. Chlorin **15** showed better stability than photochemically sensitive ferrocenyl derivative **11**. In the case of ruthenocenylchlorins, transient absorption spectroscopy provided unambiguous evidence of the successful formation of the charge-separated state, from the Rc unit (acting as an electron donor) to the singlet excited state of chlorin (acting as an electron acceptor) followed by recombination into the first excited triplet state of the chlorin unit. Additionally, the ruthenocenyl moiety had the ability to quench the triplet state formed. FMO calculations indicated that, in each structure, the HOMOs were localised in the Rcs and the LUMOs were correspondingly in the chlorins.

Experimental Section

General

All reactions were performed under argon in the dark by using standard Schlenk techniques unless otherwise noted. ^1H , ^{13}C , COSY, NOESY, HSQC and HMBC spectra were recorded at 27 °C by using Varian Mercury 300 MHz or Varian ^{UNITY}Inova 500 or 600 MHz spectrometers. ^1H and ^{13}C NMR spectra were referenced to the solvent signals (in CDCl_3 $\delta = 7.26$ and 77 ppm, respectively, and in CD_2Cl_2 $\delta = 5.32$ and 53.5 ppm, respectively). THF and CH_2Cl_2 were dried by using a Vacuum Atmospheres solvent purifier. All other solvents were obtained as HPLC quality and used as received. HRMS data were obtained on a HRMS ESI Bruker micrOTOF instrument.

Synthesis and Characterisation

The Chl *a* sample was extracted from algae, *S. pacifica*, and modified to give **1** and **2**.^[58]

Phenylchlorin 4: Compound **2** (30 mg, 0.056 mmol) was dissolved in (dry THF 10 mL); phenyllithium (0.41 mL, 1.9 M in di-*n*-butylether, 0.784 mmol) was added at –78 °C under argon. The resulting mixture was stirred at –78 °C for 2 h and allowed to warm to room temperature. The reaction was quenched by the addition of water. The reaction mixture was extracted with CH_2Cl_2 and washed with water. The solvent was evaporated and the residue was filtered through a short silica pad to give **4** (11 mg, 33%). $R_f = 0.4$ (10:1 $\text{CH}_2\text{Cl}_2/\text{MeOH}$); ^1H NMR (300 MHz, $\text{CDCl}_3/\text{CD}_3\text{OD}$): $\delta = 8.35$ (s, 1 H; 5-H), 8.16 (s, 1 H; 10-H), 7.58 (d, $^3J = 7.2$ Hz, 2 H; 2'- and 6'-H), 7.43 (s, 1 H; 20-H), 7.36 (m, $^3J_{\text{cis}} = 11.7$ Hz, $^3J_{\text{trans}} = 18.1$ Hz, 1 H; 3¹-H), 7.25–6.95 (m, 3 H; 3'-, 4'- and 5'-H), 6.59 (s, 1 H; 13²-H), 5.79 (d, $^3J_{\text{trans}} = 18.1$ Hz, 1 H; 3²_{trans}-H), 5.73 (d, $^3J_{\text{cis}} = 11.7$ Hz, 1 H; 3²_{cis}-H), 3.73 (m, 1 H; 18-H), 3.73 (m, 1 H; 17-H), 3.04 (q, $^3J = 7.5$ Hz, 2 H; 8¹-H), 2.78, 2.73 and 2.62 (each s, 3 H; 2¹-, 12¹- and 7¹-H), 2.39–1.76 (m, 4 H; 17¹- and 17²-H), 1.43 (d, $^3J = 7.1$ Hz, 3 H; 18¹-H), 1.24 ppm (t, $^3J = 7.5$ Hz, 3 H; 8²-H); HRMS (ESI-TOF): m/z calcd for $\text{C}_{39}\text{H}_{39}\text{N}_4\text{O}_2$ [$M+H$]⁺: 595.3068; found: 595.3055 ($\Delta = 2.17$ ppm).

Phenyl-substituted chlorin 5: Compound **4** (11 mg, 0.018 mmol) was dissolved in 5% $\text{H}_2\text{SO}_4/\text{MeOH}$ (10 mL) and stirred at room temperature overnight. Dichloromethane and a saturated solution of NaHCO_3 were added. The organic layer was separated and washed with water and brine. The solvent was evaporated and the crude product was purified by column chromatography on SiO_2 (1:1 hexane/EtOAc) to give **5** (8 mg, 73%). $R_f = 0.8$ (1:1 hexane/EtOAc); ^1H NMR (500 MHz, CD_2Cl_2): $\delta = 8.66$ (s, 1 H; 5-H), 8.49 (s, 1 H; 10-H), 7.85 (d, $^3J = 7.5$ Hz, 2 H; 2'- and 6'-H), 7.70 (s, 1 H; 20-H), 7.69 (dd, $^3J_{\text{cis}} = 11.7$ Hz, $^3J_{\text{trans}} = 17.8$ Hz, 1 H; 3¹-H), 7.52 (t, $^3J = 7.5$ Hz, 2 H; 3'- and 5'-H), 7.39 (t, $^3J = 7.5$ Hz, 1 H; 4'-H), 6.83 (s, 1 H; 13²-H), 6.09 (dd, $^2J_{\text{gem}} = 1.3$ Hz, $^3J_{\text{trans}} = 17.8$ Hz, 1 H; 3²_{trans}-H), 5.99 (dd, $^2J_{\text{gem}} = 1.3$ Hz, $^3J_{\text{cis}} = 11.7$ Hz, 1 H; 3²_{cis}-H), 3.95 (m, 1 H; 18-H), 3.95 (m, 1 H; 17-H), 3.70 (brs, 1 H; NH), 3.65 (s, 3 H; 17⁵-H), 3.34 (q, $^3J = 7.6$ Hz, 2 H; 8¹-H), 3.05 (s, 3 H; 2¹-H), 3.03 (s, 3 H; 12¹-H), 2.91 (s, 3 H; 7¹-H), 2.51 (m, 1 H; 17²-H), 2.51 (m, 1 H; 17¹-H), 2.37 (m, 1 H; 17²-H), 2.11 (m, 1 H; 17¹-H), 1.85 (brs, 1 H; NH), 1.66 (d, $^3J = 7.4$ Hz, 3 H; 18¹-H), 1.52 ppm (t, $^3J = 7.6$ Hz, 3 H; 8²-H); ^{13}C NMR (151 MHz, CD_2Cl_2): $\delta = 173.5$ (17³), 173.2 (19), 165.2 (16), 151.0 (6), 149.3 (9), 148.3 (14), 145.1 (1), 142.6 (8), 141.3 (11), 139.5 (13¹), 139.0 (13), 136.6 (3), 136.3 (1¹), 135.1 (4), 134.3 (7), 132.1 (13²), 130.1 (12), 129.6 (2), 129.0 (3¹), 128.5 (3' and 5'), 127.4 (4'), 126.1 (2' and 6'), 121.7 (3²), 111.8 (15), 107.1 (10), 102.5 (5), 92.6 (20), 51.5 (17⁵), 51.1 (17), 48.7 (18), 32.6 (17¹), 31.0 (17³), 22.7 (18¹), 19.0 (8¹), 17.1 (8²), 12.4 (12¹), 11.4 (2¹), 10.5 ppm

(7¹); HRMS (ESI-TOF): m/z calcd for $\text{C}_{40}\text{H}_{41}\text{N}_4\text{O}_2$ [$M+H$]⁺: 609.3224; found: 609.3242 ($\Delta = 2.96$ ppm).

Ferrocenylchlorins 7 and 8: Ferrocenyllithium was prepared from *n*-butyllithium and bromoferrocene.^[64] *n*-Butyllithium (156 μL , 2.5 M in hexane, 0.389 mmol) was added dropwise to a stirred solution of bromoferrocene (103 mg, 0.389 mmol) in dry THF (2 mL) at –78 °C under argon. The colour changed from yellow to orange upon addition. Stirring was continued at –78 °C for 15 min. Compound **2** (30 mg, 0.056 mmol) in THF (5 mL) was slowly added with a syringe. The resulting mixture was stirred at –78 °C under argon for 1 h. The cooling bath was removed and the reaction was quenched by the addition of water. Brine and CH_2Cl_2 were added and the organic layer was separated and evaporated. The crude material was filtered through a silica pad eluting first with CH_2Cl_2 to remove unreacted Fc and then with 10:1 $\text{CH}_2\text{Cl}_2/\text{methanol}$ to obtain product **7** together with undefined oxidation product **8** (overall 20 mg). **7:** $R_f = 0.6$ (10:1 $\text{CH}_2\text{Cl}_2/\text{MeOH}$); ^1H NMR (500 MHz, CD_2Cl_2): $\delta = 8.63$ (s, 1 H; 5-H), 8.50 (s, 1 H; 10-H), 7.65 (dd, $^3J_{\text{cis}} = 11.6$ Hz, $^3J_{\text{trans}} = 17.7$ Hz, 1 H; 3¹-H), 7.63 (s, 1 H; 20-H), 6.58 (s, 1 H; 13²-H), 6.09 (dd, $^2J_{\text{gem}} = 1.2$ Hz, $^3J_{\text{trans}} = 17.7$ Hz, 1 H; 3²_{trans}-H), 5.99 (dd, $^2J_{\text{gem}} = 1.2$ Hz, $^3J_{\text{cis}} = 11.6$ Hz, 1 H; 3²_{cis}-H), 4.63 (s, 2 H; 2'- and 5'-H), 4.28 (s, 2 H; 3'- and 4'-H), 4.10 (s, 5 H; 1''-H), 3.81 (m, 1 H; 18-H), 3.76 (m, 1 H; 17-H), 3.66 (brs, 1 H; NH), 3.36 (q, $^3J = 7.6$ Hz, 2 H; 8¹-H), 3.22 (s, 3 H; 12¹-H), 3.04 (s, 3 H; 2¹-H), 2.92 (s, 3 H; 7¹-H), 2.2–1.85 (m, 4 H; 17¹-17²-H), 1.88 (brs, 1 H; NH), 1.59 (d, $^3J = 7.3$ Hz, 3 H; 18¹-H), 1.55 ppm (t, $^3J = 7.6$ Hz, 3 H; 8²-H); HRMS (ESI-TOF): m/z calcd for $\text{C}_{43}\text{H}_{43}\text{FeN}_4\text{O}_2$ [$M+H$]⁺: 703.2730; found: 703.2704 ($\Delta = 3.63$ ppm).

Ferrocenylchlorins 9, 10 and 11

Procedure 1: The mixture of **7** and **8** (20 mg) was dissolved in CH_2Cl_2 (10 mL) and methanol (0.1 mL). The mixture was deoxygenated by bubbling with argon. EDC (9 mg, 0.048 mmol) and DMAP (1 mg, 0.008 mmol) were added to the solution with stirring under argon at RT. The reaction was complete after 1 h and the mixture was submitted to column chromatography on SiO_2 (10:1→1:1 hexane/ethyl acetate). A mixture of **9** and **10** (9 mg) eluted first and finally the red oxidised product **11** (5 mg, 12%; yield calculated from molar amount of **2**).

Procedure 2: Esterification was performed in a similar way to that described above in procedure 1. Purification by flash chromatography (10:1→1:1 hexane/ethylacetate) was performed by using an argon flow and eluents were bubbled with argon before use to prevent oxidation of the products. Pure brown compound **9** (4 mg) was partly purified from the mixture. In addition, an inseparable mixture of **9** and **10** (overall 11 mg) was obtained. **9:** $R_f = 0.4$ (3:1 hexane/EtOAc); ^1H NMR (500 MHz, CD_2Cl_2): $\delta = 8.66$ (s, 1 H; 5-H), 8.55 (s, 1 H; 10-H), 7.71 (dd, $^3J_{\text{cis}} = 11.6$ Hz, $^3J_{\text{trans}} = 17.7$ Hz, 1 H; 3¹-H), 7.69 (s, 1 H; 20-H), 6.71 (s, 1 H; 13²-H), 6.10 (dd, $^2J_{\text{gem}} = 1.2$ Hz, $^3J_{\text{trans}} = 17.7$ Hz, 1 H; 3²_{trans}-H), 6.01 (dd, $^2J_{\text{gem}} = 1.2$ Hz, $^3J_{\text{cis}} = 11.6$ Hz, 1 H; 3²_{cis}-H), 4.76 (s, 2 H; 2'- and 5'-H), 4.45 (s, 2 H; 3'- and 4'-H), 4.31 (s, 5 H; 1''-H), 3.93 (m, 1 H; 18-H), 3.87 (m, 1 H; 17-H), 3.66 (brs, 1 H; NH), 3.66 (s, 3 H; 17⁵-H), 3.38 (q, $^3J = 7.6$ Hz, 2 H; 8¹-H), 3.28 (s, 3 H; 12¹-H), 3.05 (s, 3 H; 2¹-H), 2.92 (s, 3 H; 7¹-H), 2.53 (m, 1 H; 17¹-H), 2.48 (m, 1 H; 17²-H), 2.38 (m, 1 H; 17²-H), 2.07 (m, 1 H; 17¹-H), 1.88 (brs, 1 H; NH), 1.66 (d, $^3J = 7.3$ Hz, 3 H; 18¹-H), 1.53 ppm (t, $^3J = 7.6$ Hz, 3 H; 8²-H); HRMS (ESI-TOF): m/z calcd for $\text{C}_{44}\text{H}_{45}\text{FeN}_4\text{O}_2$ [$M+H$]⁺: 717.2886; found: 717.2856 ($\Delta = 4.27$ ppm). **11:** $R_f = 0.1$ (3:1 hexane/EtOAc); ^1H NMR (300 MHz, CD_2Cl_2): $\delta = 11.23$ (s, 1 H; 15¹-CHO), 9.73 (s, 1 H; 10-H), 9.48 (s, 1 H; 5-H), 8.65 (s, 1 H; 20-H), 7.99

(dd, $^3J_{cis} = 11.7$ Hz, $^3J_{trans} = 17.8$ Hz, 1H; 3¹-H), 6.35 (d, $^3J_{trans} = 17.8$ Hz, 1H; 3²_{trans}-H), 6.17 (d, $^3J_{cis} = 11.7$ Hz, 1H; 3²_{cis}-H), 4.90 (m, 1H; 17-H), 4.46–4.41 (m, 4H; 2', 3', 4', 5'), 4.38 (m, 1H; 18-H), 4.05 (s, 5H; 1''), 3.73 (q, $^3J = 7.6$ Hz, 2H; 8¹-H), 3.66 (s, 3H; 12¹-H), 3.54 (s, 3H; 17⁵-H), 3.39 (s, 3H; 2¹-H), 3.22 (s, 3H; 7¹-H), 2.53 (m, 1H; 17²-H), 2.31 (m, 1H; 17¹-H), 2.23 (m, 1H; 17²-H), 1.93 (m, 1H; 17¹-H), 1.75 (d, $^3J = 7.3$ Hz, 3H; 18¹-H), 1.72 (t, $^3J = 7.6$ Hz, 3H; 8²-H), -0.22 (brs, 1H; NH), -0.29 ppm (brs, 1H; NH); ¹³C NMR (126 MHz, CD₂Cl₂): $\delta = 196.4$ (13¹), 191.2 (15¹), 173.3 (17³), 173.1 (19), 172.2 (16), 154.8 (6), 149.5 (9), 145.4 (8), 142.4 (1), 137.7 (14), 137.6 (11), 136.59 (7), 136.56 (3), 135.5 (4), 130.9 (2), 130.23 (12), 130.20 (13), 128.8 (3¹), 122.6 (3²), 106.8 (10), 105.8 (15), 102.7 (5), 94.4 (20), 84.3 (1'), 72.1 (3' and 4'), 71.1/70.8 (2' and 5'), 69.6 (1''), 52.7 (17), 51.4 (17⁵), 48.7 (18), 32.4 (17¹), 31.4 (17²), 23.5 (18¹), 19.5 (8¹), 17.4 (8²), 12.3 (12¹), 11.9 (2¹), 10.9 ppm (7¹); UV/Vis (THF): λ_{max} (%) = 697 (34), 545 (7), 506 (5), 411 nm (100); HRMS (ESI-TOF): m/z calcd for C₄₄H₄₅FeN₄O₄ [M+H]⁺: 749.2785; found: 749.2785 ($\Delta = 0.03$ ppm).

Fulvenylchlorin 12: Pyrrolidine (94 μ L, 1.16 mmol, 2 equiv) was added dropwise to a stirred mixture of **1** (317 mg, 0.58 mmol, 1 equiv) and freshly distilled cyclopentadiene (143 μ L, 1.73 mmol, 3 equiv) in THF/MeOH (1:1; 16 mL). The reaction mixture was stirred at 50 °C under argon for 4 days. Solvents were evaporated and the crude product was purified by column chromatography on SiO₂ (5:1→3:1; hexane/EtOAc, gradient) to afford yellowish brown product **12** (279 mg, 81%). $R_f = 0.8$ (1:1 hexane/EtOAc); ¹H NMR (300 MHz, CD₂Cl₂): $\delta = 9.59$ (s, 1H; 5-H), 9.53 (s, 1H; 10-H), 8.82 (s, 1H; 20-H), 8.13 (dd, $^3J_{cis} = 11.7$ Hz, $^3J_{trans} = 17.8$ Hz, 1H; 3¹-H), 7.50 (m, 1H; 2'-H), 7.15 (m, 1H; 5'-H), 6.81 (m, 1H; 3'-H), 6.78 (m, 1H; 4'-H), 6.34 (dd, $^2J_{gem} = 1.5$ Hz, $^3J_{trans} = 17.8$ Hz, 1H; 3²_{trans}-H), 6.17 (dd, $^2J_{gem} = 1.5$ Hz, $^3J_{cis} = 11.7$ Hz, 1H; 3²_{cis}-H), 5.98 (d, $^2J_{gem} = 20.0$ Hz, 1H; 13²-H), 5.84 (d, $^2J_{gem} = 20.0$ Hz, 1H; 13²-H) 4.61 (m, 1H; 18-H), 4.47 (m, 1H; 17-H), 3.72 (m, 2H; 8¹-H), 3.71 (s, 3H; 12¹-H) 3.60 (s, 3H; 17⁵-H), 3.49 (s, 3H; 2¹-H), 3.29 (s, 3H; 7¹-H), 2.77 (m, 1H; 17¹-H), 2.63 (m, 1H; 17²-H), 2.31 (m, 1H; 17¹-H), 2.31 (m, 1H; 17²-H), 1.86 (d, $^3J = 7.3$ Hz, 3H; 18¹-H), 1.72 (t, $^3J = 7.7$ Hz, 3H; 8²-H), -0.42 (brs, 1H; NH), -2.43 ppm (brs, 1H; NH); ¹³C NMR (126 MHz, CD₂Cl₂): $\delta = 173.5$ (17³), 169.3 (19), 161.5 (16), 152.9 (6), 150.8 (9), 147.2 (14), 146.2 (11), 144.3 (8), 140.0 (13), 139.8 (1), 138.0 (1'), 136.4 (7), 136.0 (12), 134.8 (3), 134.3 (4), 130.6 (3'), 130.5 (2), 130.3 (4'), 129.6 (3¹), 126.1 (13¹), 122.9 (2'), 122.3 (5'), 121.7 (3²), 108.0 (15), 101.0 (10), 97.4 (5), 93.5 (20), 52.6 (17), 51.5 (17⁵), 49.7 (18), 44.2 (13²), 30.9 (17²), 29.7 (17¹), 23.4 (18¹), 19.5 (8¹), 17.4 (8²), 15.0 (12¹), 12.1 (2¹), 11.1 ppm (7¹); HRMS (ESI-TOF): m/z calcd for C₃₉H₄₁N₄O₂ [M+H]⁺: 597.3224; found: 597.3245 ($\Delta = 3.50$ ppm).

Pentamethylruthenocenylichlorin 13: [Ru(η^5 -C₅Me₅)(η^4 -C₈H₁₂)Cl] (15 mg, 0.039 mmol) was added to a stirred mixture of fulvene **12** (23 mg, 0.039 mmol) and TEA (5 μ L, 0.039 mmol) in THF (3 mL). Reaction mixture was stirred at RT under argon for 20 min. The reaction mixture was submitted to column chromatography on SiO₂. Purification by flash chromatography (3:1 hexane/EtOAc) was performed under an argon flow and the eluent was bubbled with argon before use to prevent oxidation of product **13**. The product fraction was quickly evaporated to dryness and dried under vacuum to give brown product **13** (29 mg, 91%). The air-sensitive product was characterised immediately. ¹H NMR (500 MHz, CD₂Cl₂): $\delta = 8.56$ (s, 1H; 5-H), 8.43 (s, 1H; 10-H), 7.65 (dd, $^3J_{cis} = 11.7$ Hz, $^3J_{trans} = 17.8$ Hz, 1H; 3¹-H), 7.64 (s, 1H; 20-H), 6.50 (s, 1H; 13²-H), 6.06 (d, $^3J_{trans} = 17.8$ Hz, 1H; 3²_{trans}-H), 5.96 (d, $^3J_{cis} = 11.7$ Hz, 1H; 3²_{cis}-H), 4.86 and 4.82 (each s, 1H; 2'- and 5'-H), 4.43 (s, 2H; 3'- and 4'-H), 3.91 (m, 1H; 18-H), 3.86 (m, 1H; 17-H), 3.70 (brs, 1H; NH), 3.66 (s, 3H; 17⁵-H), 3.33 (q, $^3J = 7.6$ Hz, 2H; 8¹-H), 3.09 (s, 3H; 12¹-H),

3.02 (s, 3H; 2¹-H), 2.88 (s, 3H; 7¹-H), 2.54–2.42 (m, 1H; 17²-H), 2.54–2.42 (m, 1H; 17¹-H), 2.38–2.30 (m, 1H; 17²-H), 2.18–2.09 (m, 1H; 17²-H), 1.94 (s, 15H; 2''-H), 1.94 (brs, 1H; NH), 1.67 (d, $^3J = 7.2$ Hz, 3H; 18¹-H), 1.53 ppm (t, $^3J = 7.7$ Hz, 3H; 8²-H); ¹³C NMR (126 MHz, CD₂Cl₂): $\delta = 173.5$ (17³), 172.3 (19), 162.8 (16), 151.0 (6), 148.8 (9), 148.3 (14), 144.9 (1), 142.5 (8), 140.7 (11), 139.8 (13), 136.2 (3), 136.0 (13¹), 135.4 (4), 133.8 (7), 129.6 (2), 129.04 (3¹), 128.95 (12), 125.9 (13²), 121.4 (3²), 113.5 (15), 106.8 (10), 101.5 (5), 92.3 (20), 85.5 (1''), 83.9 (1'), 73.5 (3' and 4'), 71.6 and 71.3 (4' and 5'), 51.5 (17⁵), 50.8 (17), 48.7 (18), 32.0 (17¹), 30.9 (17²), 22.6 (18¹), 19.0 (8¹), 17.1 (8²), 13.4 (12¹), 11.43 (2''), 11.43 (2¹), 10.4 ppm (7¹); HRMS (ESI-TOF): m/z calcd for C₄₉H₅₅N₄O₂Ru [M+H]⁺: 833.3363; found: 833.3343 ($\Delta = 2.46$ ppm).

Pentamethylruthenocenylichlorins (R)-14, (S)-14 and 15: [Ru(η^5 -C₅Me₅)(η^4 -C₈H₁₂)Cl] (16 mg, 0.042 mmol) was added to a stirred mixture of fulvene **12** (25 mg, 0.042 mmol) and TEA (5 μ L, 0.042 mmol) in THF (3 mL). The reaction mixture was stirred at RT under argon for 20 min until product **13** had formed and there was no starting material left. Then the reaction mixture was stirred in air for 10 min until **13** had fully oxidised to give compounds (R)-**14** and **15**. These products were separated by column chromatography on SiO₂ (10:1→1:1 hexane/EtOAc) eluting first green compounds (R)- and (S)-**14** separately and finally red compound **15**. (R)-**14**: Yield: ≈ 8 mg, 0.0094 mmol, 22%; $R_f = 0.7$ (3:1 hexane/EtOAc); ¹H NMR (500 MHz, CDCl₃): $\delta = 9.80$ (s, 1H; 5-H), 9.46 (s, 1H; 10-H), 8.79 (s, 1H; 20-H), 8.12 (dd, $^3J_{cis} = 11.7$ Hz, $^3J_{trans} = 17.8$ Hz, 1H; 3¹-H), 6.28 (d, $^3J_{trans} = 17.8$ Hz, 1H; 3²_{trans}-H), 6.14 (d, $^3J_{cis} = 11.7$ Hz, 1H; 3²_{cis}-H), 5.42 (s, 1H; 13¹-H), 4.99 (m, 1H; 17-H), 4.91 (s, 1H; 2'), 4.72 (s, 1H; 5'), 4.53 (m, 1H; 18-H), 4.20 (s, 1H; 3'), 4.16 (s, 1H; 4'), 3.74 (q, $^3J = 7.6$ Hz, 2H; 8¹-H), 3.63 (s, 3H; 17⁵-H), 3.59 (s, 3H; 12¹-H), 3.45 (s, 3H; 2¹-H), 3.31 (s, 3H; 7¹-H), 2.88 (m, 1H; 17¹-H), 2.76 (m, 1H; 17²-H), 2.45 (m, 1H; 17²-H), 2.30 (m, 1H; 17¹-H), 1.84 (s, 15H; 2''), 1.76 (d, $^3J = 7.2$ Hz, 3H; 18¹-H), 1.71 (t, $^3J = 7.6$ Hz, 3H; 8²-H), 0.24 (brs, 1H; NH), -1.70 ppm (brs, 1H; NH); ¹³C NMR (126 MHz, CDCl₃): $\delta = 203.3$ (13²), 173.8 (17³), 169.0 (19), 168.7 (16), 152.5 (9), 151.6 (14), 148.9 (6), 142.3 (8), 140.1 (11), 138.8 (1), 137.5 (7), 136.6 (13), 135.2 (3), 130.8 (4), 129.8 (3¹), 128.3 (12), 127.4 (2), 121.7 (3²), 105.7 (15), 104.6 (5), 101.1 (10), 95.7 (20), 89.2 (1'), 85.3 (1''), 73.0 (4'), 72.6 (2'), 72.4 (3'), 71.4 (5'), 53.6 (17), 51.5 (17⁵), 48.0 (13¹), 47.7 (18), 32.2 (17²), 30.9 (17¹), 24.2 (18¹), 19.5 (8¹), 17.6 (8²), 13.0 (12¹), 12.1 (2¹), 11.9 (2''), 11.3 ppm (7¹); UV/Vis (THF): λ_{max} (%) = 666 (32), 534 (6), 499 (7), 400 nm (100); HRMS (ESI-TOF): m/z calcd for C₄₉H₅₅N₄O₃Ru [M+H]⁺: 849.3312; found: 849.3295 ($\Delta = 2.04$ ppm). (S)-**14**: Yield: ≈ 8 mg, 0.0094 mmol, 22%; $R_f = 0.6$ (3:1 hexane/EtOAc); ¹H NMR (500 MHz, CDCl₃): $\delta = 9.82$ (s, 1H; 5-H), 9.52 (s, 1H; 10-H), 8.82 (s, 1H; 20-H), 8.11 (dd, $^3J_{cis} = 11.7$ Hz, $^3J_{trans} = 17.8$ Hz, 1H; 3¹-H), 6.28 (d, $^3J_{trans} = 17.8$ Hz, 1H; 3²_{trans}-H), 6.15 (d, $^3J_{cis} = 11.7$ Hz, 1H; 3²_{cis}-H), 5.63 (s, 1H; 13¹-H), 5.07 (s, 1H; 2'), 5.03 (m, 1H; 17-H), 4.83 (s, 1H; 5'), 4.51 (m, 1H; 18-H), 4.24 (s, 1H; 3'), 4.20 (s, 1H; 4'), 3.76 (q, $^3J = 7.5$ Hz, 2H; 8¹-H), 3.65 (s, 3H; 12¹-H), 3.52 (s, 3H; 17⁵-H), 3.46 (s, 3H; 2¹-H), 3.33 (s, 3H; 7¹-H), 2.63 (m, 1H; 17¹-H), 2.63 (m, 1H; 17²-H), 2.19 (m, 1H; 17²-H), 2.19 (m, 1H; 17¹-H), 1.84 (d, $^3J = 6.6$ Hz, 3H; 18¹-H), 1.75 (t, $^3J = 7.5$ Hz, 3H; 8²-H) 1.46 (s, 15H; 2''), 0.26 (brs, 1H; NH), 1.68 ppm (brs, 1H; NH); ¹³C NMR (126 MHz, CDCl₃): $\delta = 202.7$ (13²), 173.8 (17³), 168.9 (19), 168.8 (16), 152.5 (9), 152.1 (14), 149.0 (6), 142.4 (8), 140.1 (11), 138.8 (1), 137.6 (7), 135.6 (13), 135.3 (3), 130.8 (4), 129.7 (3¹), 128.6 (12), 127.4 (2), 121.8 (3²), 104.2 (15), 103.9 (5), 101.1 (10), 95.8 (20), 88.3 (1'), 85.0 (1''), 72.9 (3'), 72.64 (4'), 72.58 (2'), 71.6 (5'), 53.5 (17), 51.4 (17⁵), 47.9 (13¹), 47.8 (18), 31.7 (17²), 30.4 (17¹), 24.4 (18¹), 19.6 (8¹), 17.6 (8²), 13.4 (12¹), 12.1 (2¹), 11.6 (2''), 11.3 ppm (7¹); UV/Vis (THF): λ_{max} (%) = 666 (32), 533 (5), 499 (6), 400 nm (100); HRMS (ESI-TOF):

m/z calcd for $C_{49}H_{55}N_4O_3Ru$ $[M+H]^+$: 849.3312; found: 849.3301 ($\Delta = 1.30$ ppm). **15**: Yield: 5 mg, 0.0058 mmol, 14%; $R_f = 0.2$ (3:1 hexane/EtOAc); 1H NMR (500 MHz, $CDCl_3$): $\delta = 11.42$ (s, 1H; 15^1 -CHO), 9.64 (s, 1H; 10-H), 9.41 (s, 1H; 5-H), 8.57 (s, 1H; 20-H), 7.93 (dd, $^3J_{cis} = 11.7$ Hz, $^3J_{trans} = 17.8$ Hz, 1H; 3^1 -H), 6.30 (d, $^3J_{trans} = 17.8$ Hz, 1H; 3^2_{trans} -H), 6.14 (d, $^3J_{cis} = 11.7$ Hz, 1H; 3^2_{cis} -H), 4.94 (m, 1H; 17-H), 4.46–4.24 (m, 4H; 2^- , 3^- , 4^- , 5^- -H), 4.34 (m, 1H; 18-H), 3.70 (q, $^3J = 7.7$ Hz, 2H; 8^1 -H), 3.68 (s, 3H; 12^1 -H), 3.59 (s, 3H; 17^5 -H), 3.36 (s, 3H; 2^1 -H), 3.20 (s, 3H; 7^1 -H), 2.67–1.93 (m, 4H; 17^1 - 17^2 -H), 1.73 (s, 15H; $2''$), 1.69 (d, $^3J = 7.3$ Hz, 3H; 18^1 -H), 1.69 (t, $^3J = 7.7$ Hz, 3H; 8^2 -H), -0.26 ppm (brs, 2H; NH); ^{13}C NMR (126 MHz, $CDCl_3$): $\delta = 193.7$ (13^1), 189.8 (15^1), 173.7 (17^3), 173.5 (19), 172.0 (16), 154.7 (6), 149.3 (9), 145.2 (8), 142.2 (1), 139.9 (14), 137.6 (11), 136.4 (3), 136.2 (7), 135.4 (4), 130.4 (2), 130.1 (12), 129.6 (13), 128.9 (3^1), 122.6 (3^2), 106.8 (15), 106.5 (10), 102.4 (5), 94.2 (20), 90.2 (1^1), 86.4 ($1''$), 76.1, 75.1, 74.7 (2^1 , 3^1 , 4^1 , 5^1), 53.3 (17), 51.5 (17^5), 48.7 (18), 32.1 (17^2), 31.9 (17^1), 23.9 (18^1), 19.5 (8^1), 17.6 (8^2), 12.6 (12^1), 12.0 (2^1), 11.7 ($2''$), 11.1 ppm (7^1); UV/Vis (THF): λ_{max} (%) = 700 (37), 549 (9), 507 (8), 413 nm (100); HRMS (ESI-TOF): m/z calcd for $C_{49}H_{55}N_4O_3Ru$ $[M+H]^+$: 865.3261; found: 865.3239 ($\Delta = 2.63$ ppm).

Photochemistry and electrochemistry

Steady-state UV/Vis absorption spectra were measured on Cary5000 (Varian) and Perkin-Elmer Lambda 2 two-beam spectrophotometers. Steady-state fluorescence spectra were recorded on samples with a FluoroMax3 spectrometer (Horiba Jobin Yvon). The experiments were performed at room temperature. Fluorescence quantum yields were determined by the comparative method by using *meso*-tetraphenylporphyrin (TPP; $\Phi_f = 0.11$ in toluene^[84]) as a standard. Fluorescence lifetimes were determined with the time-correlated single-photon-counting technique by using a Fluorolog 3 instrument (Horiba Jobin Yvon). The sample was excited by using a NanoLED-405 LH ($\lambda = 403$ nm) and the signal was detected by using a Hamamatsu MCP photomultiplier (type R3809U-50). The time profiles were recorded at $\lambda = 670$ nm.

Transient absorption measurements based on femtosecond laser photolysis were performed with the output from an amplified Ti:Sapphire laser system (CPA-2101 and CPA-2110 from Clark-MXR Inc.): 1 kHz, 150 fs full-width at half-maximum (FWHM) pulses, and the laser energy was 200 nJ. The excitation wavelength was generated by second-harmonic generation ($\lambda = 387$ nm). Nanosecond transient absorption experiments were performed with an EOS spectrometer (Ultrafast Systems LLC). The pump pulses at $\lambda = 387$ nm were from the amplified Ti:Sapphire laser system described above. The probe pulse (2 kHz, 0.5 ns pulse width), which was generated in a photonic fiber, was synchronised with the femtosecond amplifier.

Electrochemical experiments were carried out with a Metrohm FRA 2 μ Autolab Type III potentiostat in THF containing 0.1 M TBAPF₆ (TBA = tetrabutylammonium) as the supporting electrolyte. A single-compartment, three-electrode cell configuration was used in this work. A glassy carbon electrode (3 mm diameter) was used as the working electrode, a platinum wire was the counter electrode and an Ag wire was the reference electrode. All potentials were corrected against the ferrocene couple (Fc/Fc^+) internal reference. Spectroelectrochemical experiments were performed with a homemade setup containing a potentiostat (Metrohm Autolab PGSTAT 101) and Analytik Jena Specord absorption spectrophotometer. The working electrode was a platinum gauze (99.9%, 1024 mesh/cm², 0.06 mm wire diameter) from ChemPur, platinum

wire was used as the counter electrode and Ag wire was used as the reference electrode.

Computational details

The ring-current susceptibilities, denoted in the following as ring-current strengths, for chlorins **1** and **5** were obtained by using the GIMIC method.^[85] The GIMIC program used the magnetically perturbed and unperturbed electron densities obtained from a calculation of NMR shieldings to calculate the ring-current strengths. The prerequisite NMR shielding calculations were performed at the DFT level by using Becke's three-parameter functional combined with the Lee–Yang–Parr exchange-correlation functional (B3LYP)^[86,87] and the def2-SVP basis set^[88] in the Turbomole 6.5^[89] program. For closed-shell molecules with only light elements, this level of theory has been proven to give accurate ring currents.^[76] The ring-current strengths were obtained by numerical integration of the current density passing through cut planes placed at the mid-point of a bond perpendicular to the bond. NICS^[77] values at the centre of the macrocycle and at the centre of the five-membered rings in the molecular plane (NICS(0)) were obtained at the same B3LYP/def2-SVP level as the current strengths. Current-pathway pictures were drawn with GABEDIT and GIMP software.^[90] The geometries for FMO calculations were optimised with the TPSS-D3-BJ functional, def2-SVP basis set and COSMO solvation model with the dielectric constant of chloroform ($\epsilon = 4.7$).^[91] The dispersion corrections were calculated with the D3 method by using Becke and Johnson (BJ) damping.^[92]

Acknowledgements

Sincere gratitude to Dr. Sami Heikkinen for his assistance in NMR spectroscopy measurements and Dr. Petri Heinonen for the HRMS measurements. T.N. gratefully acknowledges the Graduate School of Organic Chemistry and Chemical Biology (GSOCCB) and the Finnish Cultural Foundation for financial support. M.M.O. acknowledges financial support from the Marie Curie COFUND programme "U-Mobility" co-financed by the Universidad de Malaga and the European Community's Seventh Framework Program under Grant Agreement No. 246550. A.K. gratefully acknowledges funding from the Deutsche Forschungsgemeinschaft (DFG) through Grant KA 3491/2-1. Funding from the Bayerische Staatsregierung as part of the "Solar Technologies go Hybrid" initiative is gratefully acknowledged. Special thanks are due to Prof. Dirk M. Guldi (Friedrich-Alexander-Universität Erlangen-Nürnberg) for his support during the photochemical and electrochemical measurements and advice for preparing this manuscript. Financial support from the Academy of Finland (project no. (S.T.) 1268251 and (J.H.) 129062) is acknowledged. The Finnish National Centre for Scientific Computing (CSC) is recognised for computational resources.

Keywords: aromaticity • donor–acceptor systems • electron transfer • metallocenes • photochemistry

[1] A. N. Melkozernov, R. E. Blankenship, *Photosynthetic Functions of Chlorophylls. In Advances in Photosynthesis and Respiration - Chlorophylls and Bacteriochlorophylls: Biochemistry Biophysics, Functions and Applications*,

- (Eds.: B. Grimm, R. J. Porra, W. Rüdiger, H. Scheer), Springer, Heidelberg, **2006**, Vol. 25, pp. 397–412.
- [2] S. Fukuzumi, K. Ohkubo, H. Imahori, J. Shao, Z. Ou, G. Zheng, Y. Chen, R. K. Pandey, M. Fujitsuka, O. Ito, K. M. Kadish, *J. Am. Chem. Soc.* **2001**, *123*, 10676–10683.
 - [3] A. R. Holzwarth, M. Katterle, M. G. Müller, Y.-Z. Ma, V. Prokhorenko, *Pure Appl. Chem.* **2001**, *73*, 469–474.
 - [4] J. S. Kavakka, S. Heikkinen, I. Kilpeläinen, M. Mattila, H. Lipsanen, J. Helaja, *Chem. Commun.* **2007**, 519–521.
 - [5] J. S. Kavakka, S. Heikkinen, I. Kilpeläinen, N. V. Tkachenko, J. Helaja, *Chem. Commun.* **2009**, 758–760.
 - [6] T. Nikkonen, M. Moreno Oliva, A. Kahnt, M. Muuronen, J. Helaja, D. M. Guldi, *Chem. Eur. J.* **2015**, *21*, 590–600.
 - [7] F.-P. Montforts, O. Kutzki, *Angew. Chem. Int. Ed.* **2000**, *39*, 599–601; *Angew. Chem.* **2000**, *112*, 612–614.
 - [8] K. Ohkubo, H. Kotani, J. Shao, Z. Ou, K. M. Kadish, G. Li, R. K. Pandey, M. Fujitsuka, O. Ito, H. Imahori, S. Fukuzumi, *Angew. Chem. Int. Ed.* **2004**, *43*, 853–856; *Angew. Chem.* **2004**, *116*, 871–874.
 - [9] K. Stranius, V. Iashin, T. Nikkonen, M. Muuronen, J. Helaja, N. Tkachenko, *J. Phys. Chem. A* **2014**, *118*, 1420–1429.
 - [10] N. V. Tkachenko, L. Rantala, A. Y. Tauber, J. Helaja, P. H. Hynninen, H. Lemmetyinen, *J. Am. Chem. Soc.* **1999**, *121*, 9378–9387.
 - [11] M. R. Wasielewski, G. P. Wiederrecht, W. A. Svec, M. P. Niemczyk, *Sol. Energy Mater. Sol. Cells* **1995**, *38*, 127–134.
 - [12] V. Vehmanen, N. V. Tkachenko, A. Y. Tauber, P. H. Hynninen, H. Lemmetyinen, *Chem. Phys. Lett.* **2001**, *345*, 213–218.
 - [13] M. J. Pellin, K. J. Kaufmann, M. R. Wasielewski, *Nature* **1979**, *278*, 54–55.
 - [14] M. R. Wasielewski, R. L. Smith, A. G. Kostka, *J. Am. Chem. Soc.* **1980**, *102*, 6923–6928.
 - [15] J. Fajer, D. C. Brune, M. S. Davis, A. Forman, L. D. Spaulding, *Proc. Natl. Acad. Sci. USA* **1975**, *72*, 4956–4960.
 - [16] M. Morisue, D. Kalita, N. Haruta, Y. Kobuke, *Chem. Commun.* **2007**, 2348–2350.
 - [17] K. Uosaki, T. Kondo, X.-Q. Zhang, M. Yanagida, *J. Am. Chem. Soc.* **1997**, *119*, 8367–8368.
 - [18] R. Giasson, E. J. Lee, X. Zhao, M. S. Wrighton, *J. Phys. Chem.* **1993**, *97*, 2596–2601.
 - [19] S. Fery-Forgues, B. Delavaux-Nicot, *J. Photochem. Photobiol. A* **2000**, *132*, 137–159.
 - [20] R. W. Wagner, P. A. Brown, T. E. Johnson, J. S. Lindsey, *J. Chem. Soc. Chem. Commun.* **1991**, 1463–1466.
 - [21] L. Lvova, P. Galloni, B. Floris, I. Lundström, R. Paolesse, C. Di Natale, *Sensors* **2013**, *13*, 5841–5856.
 - [22] C. Bucher, C. H. Devillers, J.-C. Moutet, G. Royal, E. Saint-Aman, *Coord. Chem. Rev.* **2009**, *253*, 21–36.
 - [23] J.-J. Oviedo, M. E. El-Khouly, P. de La Cruz, L. Pérez, J. Garín, J. Orduna, Y. Araki, F. Langa, O. Ito, *New J. Chem.* **2006**, *30*, 93–101.
 - [24] D. M. Guldi, G. M. A. Rahman, R. Marczak, Y. Matsuo, M. Yamanaka, E. Nakamura, *J. Am. Chem. Soc.* **2006**, *128*, 9420–9427.
 - [25] S.-H. Lee, A. G. Larsen, K. Ohkubo, Z.-L. Cai, J. R. Reimers, S. Fukuzumi, M. J. Crossley, *Chem. Sci.* **2012**, *3*, 257–269.
 - [26] H. Imahori, S. Fukuzumi, *Adv. Funct. Mater.* **2004**, *14*, 525–536.
 - [27] B. M. J. M. Suijkerbuijk, R. J. M. Klein Gebbink, *Angew. Chem. Int. Ed.* **2008**, *47*, 7396–7421; *Angew. Chem.* **2008**, *120*, 7506–7532.
 - [28] A. N. Cammidge, P. J. Scaife, G. Berber, D. L. Hughes, *Org. Lett.* **2005**, *7*, 3413–3416.
 - [29] R. G. Wollmann, D. N. Hendrickson, *Inorg. Chem.* **1977**, *16*, 3079–3089.
 - [30] O. Shoji, S. Okada, A. Satake, Y. Kobuke, *J. Am. Chem. Soc.* **2005**, *127*, 2201–2210.
 - [31] P. Jutzl, N. Burford, *Main Group Metalloenes. In Metalloenes* (Eds.: A. Togni, R. L. Halterman), Wiley-VCH, Weinheim, **1998**, Vol. 1, pp. 1–54.
 - [32] J. Bennewitz, M. Nieger, B. Lewall, K. H. Dötz, *J. Organomet. Chem.* **2005**, *690*, 5892–5899.
 - [33] H. J. H. Wang, L. Jaquinod, D. J. Nurco, M. G. H. Vicente, K. M. Smith, *Chem. Commun.* **2001**, 2646–2647.
 - [34] H. J. H. Wang, L. Jaquinod, M. M. Olmstead, M. G. H. Vicente, K. M. Kadish, Z. Ou, K. M. Smith, *Inorg. Chem.* **2007**, *46*, 2898–2913.
 - [35] E. D. Bergmann, *Chem. Rev.* **1968**, *68*, 41–84.
 - [36] G. Erker, *Coord. Chem. Rev.* **2006**, *250*, 1056–1070.
 - [37] K. M. Kane, P. J. Shapiro, A. Vij, R. Cubbon, A. L. Rheingold, *Organometallics* **1997**, *16*, 4567–4571.
 - [38] J. J. Eisch, X. Shi, F. A. Ownor, *Organometallics* **1998**, *17*, 5219–5221.
 - [39] J. J. Eisch, F. A. Owuor, X. Shi, *Polyhedron* **2005**, *24*, 1325–1339.
 - [40] R. C. Kerber, D. J. Ehntholt, *Synthesis* **1970**, 449–465.
 - [41] R. P. Hughes, D. J. Robinson, *Organometallics* **1989**, *8*, 1015–1019.
 - [42] R. P. Hughes, H. A. Trujillo, A. J. Gauri, *Organometallics* **1995**, *14*, 4319–4324.
 - [43] S. K. S. Tse, T. Guo, H. H.-Y. Sung, I. D. Williams, Z. Lin, G. Jia, *Organometallics* **2009**, *28*, 5529–5535.
 - [44] M. Sato, Y. Kawata, H. Shintate, Y. Habata, S. Akabori, K. Unoura, *Organometallics* **1997**, *16*, 1693–1701.
 - [45] M. Sato, A. Iwai, M. Watanabe, *Organometallics* **1999**, *18*, 3208–3219.
 - [46] J. C. Swarts, A. Nafady, J. H. Roudebush, S. Trubia, W. E. Geiger, *Inorg. Chem.* **2009**, *48*, 2156–2165.
 - [47] E. Erasmus, J. C. Swarts, *New J. Chem.* **2013**, *37*, 2862–2873.
 - [48] T. Kuwana, D. E. Bublitz, G. Hoh, *J. Am. Chem. Soc.* **1960**, *82*, 5811–5817.
 - [49] L. I. Denisovich, N. V. Zakurin, A. A. Bezrukova, S. P. Gubin, *J. Organomet. Chem.* **1974**, *81*, 207–216.
 - [50] R. J. Gale, R. Job, *Inorg. Chem.* **1981**, *20*, 42–45.
 - [51] M. G. Hill, W. M. Lamanna, K. R. Mann, *Inorg. Chem.* **1991**, *30*, 4687–4690.
 - [52] U. Koelle, A. Salzer, *J. Organomet. Chem.* **1983**, *243*, C27–C30.
 - [53] K. Hashidzume, H. Tobita, H. Ogino, *Organometallics* **1995**, *14*, 1187–1194.
 - [54] H. Mansour, M. E. El-Khouly, S. Y. Shaban, O. Ito, N. Jux, *J. Porphyrins Phthalocyanines* **2007**, *11*, 719–728.
 - [55] L. Cuesta, E. Karnas, V. M. Lynch, J. L. Sessler, W. Kajonkijya, W. Zhu, M. Zhang, Z. Ou, K. M. Kadish, K. Ohkubo, S. Fukuzumi, *Chem. Eur. J.* **2008**, *14*, 10206–10210.
 - [56] L. Cuesta, E. Karnas, V. M. Lynch, P. Chen, J. Shen, K. M. Kadish, K. Ohkubo, S. Fukuzumi, J. L. Sessler, *J. Am. Chem. Soc.* **2009**, *131*, 13538–13547.
 - [57] L. Cuesta, J. L. Sessler, *J. Chem. Soc. Rev.* **2009**, *38*, 2716–2729.
 - [58] K. M. Smith, D. A. Goff, D. J. Simpson, *J. Am. Chem. Soc.* **1985**, *107*, 4946–4954.
 - [59] L. Jaquinod, M. O. Senge, R. K. Pandey, T. P. Forsyth, K. M. Smith, *Angew. Chem. Int. Ed. Engl.* **1996**, *35*, 1840–1842; *Angew. Chem.* **1996**, *108*, 1982–1984.
 - [60] S.-I. Sasaki, M. Yoshizato, M. Kunieda, H. Tamiaki, *Eur. J. Org. Chem.* **2010**, 5287–5291.
 - [61] H. Tamiaki, R. Monobe, S. Koizumi, T. Miyatake, Y. Kinoshita, *Tetrahedron: Asymmetry* **2013**, *24*, 677–682.
 - [62] T. Nikkonen, R. Haavikko, J. Helaja, *Org. Biomol. Chem.* **2009**, *7*, 2046–2052.
 - [63] S. Yagai, T. Miyatake, Y. Shimono, H. Tamiaki, *Photochem. Photobiol.* **2001**, *73*, 153–163.
 - [64] F. L. Hedberg, H. Rosenberg, *Tetrahedron Lett.* **1969**, *10*, 4011–4012.
 - [65] K. J. Stone, R. D. Little, *J. Org. Chem.* **1984**, *49*, 1849–1853.
 - [66] J. A. Varela, S. G. Rubin, L. Castedo, C. Saá, *J. Org. Chem.* **2008**, *73*, 1320–1332.
 - [67] R. Schmid, K. Kirchner, *Eur. J. Inorg. Chem.* **2004**, 2609–2626.
 - [68] M. O. Albers, D. J. Robinson, A. Shaver, E. Singleton, *Organometallics* **1986**, *5*, 2199–2205.
 - [69] P. H. Hynninen, *Chemistry of Chlorophylls: Modifications. In Chlorophylls* (Ed. H. Scheer), CRC Press, Boca Raton, **1991**, pp. 145–209.
 - [70] P. H. Hynninen, M. R. Wasielewski, J. J. Katz, *Acta Chem. Scand.* **1979**, *33*, 637–648.
 - [71] S. Löfjón, P. H. Hynninen, *Acta Chem. Scand.* **1990**, *44*, 235–238.
 - [72] L. Ma, D. Dolphin, *Tetrahedron Lett.* **1995**, *36*, 7791–7794.
 - [73] L. Ma, D. Dolphin, *Can. J. Chem.* **1997**, *75*, 262–275.
 - [74] J. Li, J.-P. Ma, F. Liu, X.-W. Wu, Y.-B. Dong, R.-Q. Huang, *Organometallics* **2008**, *27*, 5446–5452.
 - [75] H. Scheer, J. J. Katz, *J. Am. Chem. Soc.* **1975**, *97*, 3273–3275.
 - [76] H. Fliegl, D. Sundholm, *J. Org. Chem.* **2012**, *77*, 3408–3414.
 - [77] P. von Ragué Schleyer, C. Maerker, A. Dransfeld, H. Jiao, N. J. R. van Eike-Hommes, *J. Am. Chem. Soc.* **1996**, *118*, 6317–6318.
 - [78] H. Fliegl, N. Özcan, R. Mera-Adasme, F. Pichierri, J. Jusélius, D. Sundholm, *Mol. Phys.* **2013**, *111*, 1364–1372.
 - [79] C. Geskes, M. Meyer, M. Fischer, H. Scheer, J. Heinze, *J. Phys. Chem.* **1995**, *99*, 17669–17672.
 - [80] D. M. Niedzwiedzki, R. E. Blankenship, *Photosynth. Res.* **2010**, *106*, 227–238.

- [81] H. L. Kee, C. Kirmaier, Q. Tang, J. R. Diers, C. Muthiah, M. Taniguchi, J. K. Laha, M. Ptaszek, J. S. Lindsey, D. F. Bocian, D. Holten, *Photochem. Photobiol.* **2007**, *83*, 1110–1124.
- [82] S. Al-Omari, *Romanian J. Biophys.* **2010**, *20*, 295–314.
- [83] Y. Takahashi, Ö. Hansson, P. Mathis, K. Satoh, *Biochim. Biophys. Acta* **1987**, *893*, 49–59.
- [84] P. G. Seybold, M. Gouterman, *J. Mol. Spectrosc.* **1969**, *31*, 1–13.
- [85] J. Jusélius, D. Sundholm, J. Gauss, *J. Chem. Phys.* **2004**, *121*, 3952–3963.
- [86] A. D. Becke, *J. Chem. Phys.* **1993**, *98*, 5648–5652.
- [87] C. Lee, W. Yang, R. G. Parr, *Phys. Rev. B* **1988**, *37*, 785–789.
- [88] F. Weigend, R. Ahlrichs, *Phys. Chem. Chem. Phys.* **2005**, *7*, 3297–3305.
- [89] R. Ahlrichs, M. Bär, M. Häser, H. Horn, C. Kölmel, *Chem. Phys. Lett.* **1989**, *162*, 165–169.
- [90] A. R. Allouche, *J. Comput. Chem.* **2011**, *32*, 174–182.
- [91] A. Schäfer, A. Klamt, D. Sattel, J. C. W. Lohrenz, F. Eckert, *Phys. Chem. Chem. Phys.* **2000**, *2*, 2187–2193.
- [92] S. Grimme, S. Ehrlich, L. Goerigk, *J. Comput. Chem.* **2011**, *32*, 1456–1465.

Received: May 12, 2015

Published online on July 29, 2015